DOI: 10.1002/anie.201306588

Nanostructured Electrocatalysts

Oxygen Electrochemistry as a Cornerstone for Sustainable Energy Conversion

Ioannis Katsounaros, Serhiy Cherevko, Aleksandar R. Zeradjanin, and Karl J. J. Mayrhofer**

Keywords:
electrolysis · fuel cells · nanostructures · oxygen evolution · oxygen reduction

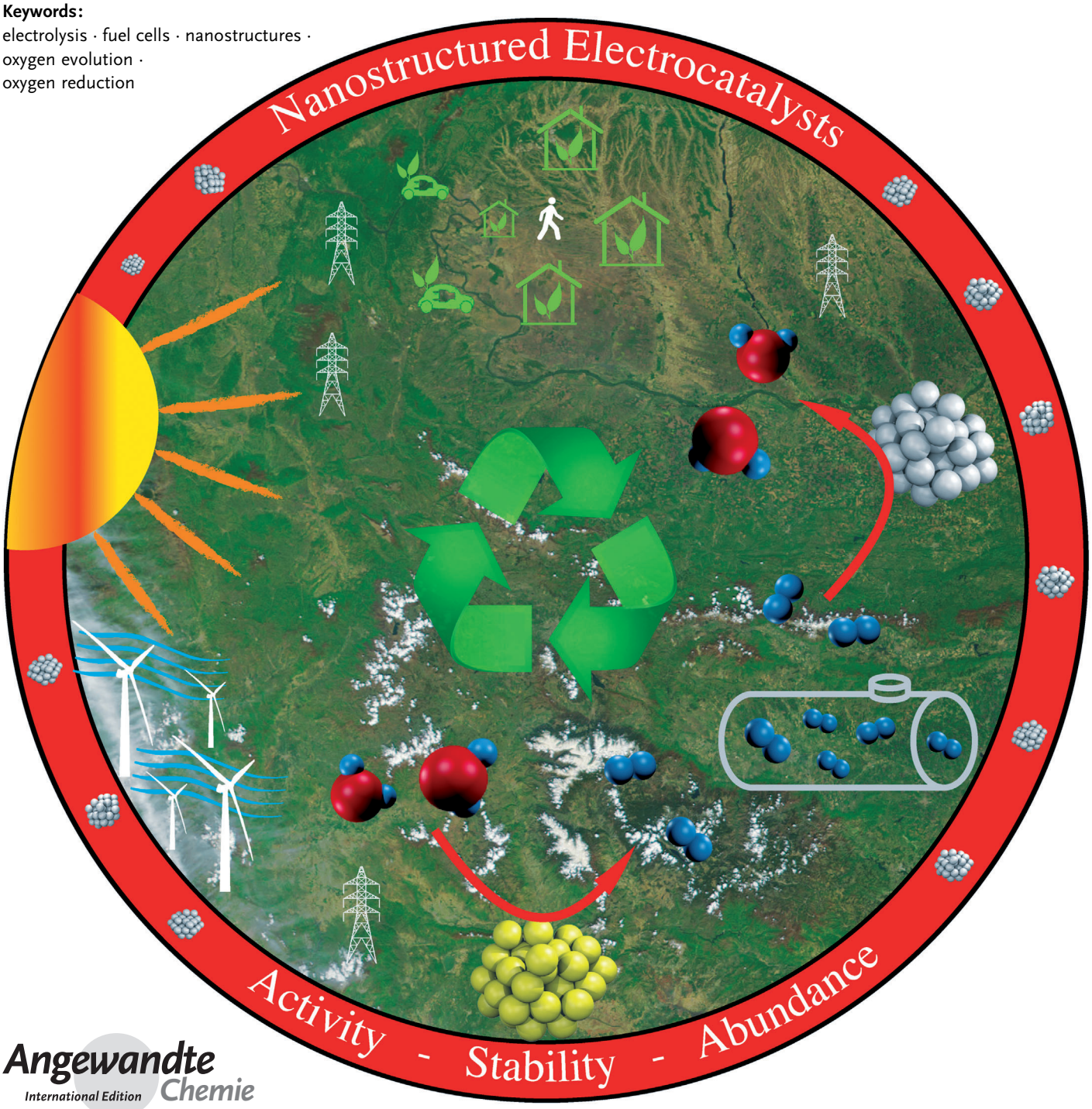

Electrochemistry will play a vital role in creating sustainable energy solutions in the future, particularly for the conversion and storage of electrical into chemical energy in electrolysis cells, and the reverse conversion and utilization of the stored energy in galvanic cells. The common challenge in both processes is the development of—preferably abundant—nanostructured materials that can catalyze the electrochemical reactions of interest with a high rate over a sufficiently long period of time. An overall understanding of the related processes and mechanisms occurring under the operation conditions is a necessity for the rational design of materials that meet these requirements. A promising strategy to develop such an understanding is the investigation of the impact of material properties on reaction activity/selectivity and on catalyst stability under the conditions of operation, as well as the application of complementary in situ techniques for the investigation of catalyst structure and composition.

From the Contents

1. Introduction 103

2. Fundamental Aspects of the Reactions of Interest 104

3. Catalysis of the Electrochemical Oxygen Reduction Reaction (ORR) 105

4. Catalysis of the Electrochemical Oxygen Evolution Reaction (OER) 110

5. Outlook and Future Challenges 115

1. Introduction

Finding sustainable solutions to the looming energy crisis on both the small and large scale has become one of the most urgent challenges on the way to reduce our dependence on conventional energy sources based on fossil fuels.[1,2] Over the last few years, several technologies that provide electrical energy from renewable sources (e.g. solar photovoltaics, wind power generators etc) have been increasingly implemented.[3] However, the supply of energy from such sources is intermittent, and since the usage of electricity fluctuates independently this leads to a continuous mismatch between supply and demand. Therefore, to provide integrated solutions, such technologies must be coupled with advanced energy conversion and storage processes.[2–4] In this framework, electrochemistry plays an essential role, as it allows transformations between electrical and chemical energy and vice versa, thereby enabling the storage of energy in the form of chemical bonds. This is broadly termed electrochemical energy conversion and storage.[5] In particular, when the supply from renewable sources exceeds the demand, the electrical energy surplus can be used to carry out nonspontaneous electrochemical reactions (in electrolysis cells) and stored in the more convenient form of chemical energy. At times when the supply does not meet the demand, the energy deficit can be covered by converting the previously stored chemical energy into electrical energy through spontaneous electrochemical reactions occurring in galvanic cells.

Although rechargeable batteries are already commonly used for energy conversion for small-scale portable applications (e.g. in mobile phones, laptops, or even cars) in commercially available devices,[6] other approaches based on continuous electrolysis and galvanic reactors for large-scale applications still require major research efforts to reach this state. For example, the reduction of carbon dioxide as an initial reactant to produce either fuels directly (e.g. methanol) or precursors for the formation of fuels (e.g. synthetic gas) seems promising for large-scale applications ("methanol economy").[7] Even though this carbon cycle includes the advantage of the easy storage and transportation of a liquid fuel using the existing infrastructure, there is still a high demand for fundamental research on the selective reductive conversion of carbon dioxide with high activity as well as the reverse oxidation process.[8,9] Much more interest has so far been devoted to energy conversion based on the hydrogen cycle ("hydrogen economy").[10] In this case, water splitting is used as the initial reaction, which leads to the evolution of hydrogen at the cathode [Eq. (1)] and of oxygen at the anode [Eq. (2)] of the electrolyzer (the reactions are shown for acidic media).

$$4\,H^+ + 4\,e^- \rightleftharpoons 2\,H_2 \quad (1)$$

$$2\,H_2O \rightleftharpoons O_2 + 4\,H^+ + 4\,e^- \quad (2)$$

The hydrogen fuel produced can thereafter be oxidized at the anode [reverse reaction to Eq. (1)] during times of high demand, while the counter reaction is the reduction of oxygen that takes place at the cathode [reverse reaction to Eq. (2)] of a H_2/air fuel cell. It is nowadays well established that the hydrogen evolution and oxidation reactions proceed at a high rate, for example, on platinum-based catalysts.[11] The bottleneck, particularly in acidic media at low temperature is actually the development of materials for the catalysis of the electrochemical oxygen reactions, namely the oxygen evolution reaction—OER (in electrolyzers) and the oxygen reduction reaction—ORR (in fuel cells).

Highly dispersed, nanostructured electrocatalysts are typically used to increase the surface-to-volume ratio and

[*] Dr. I. Katsounaros, Dr. S. Cherevko, Dr. A. R. Zeradjanin, Dr. K. J. J. Mayrhofer
Department of Interface Chemistry and Surface Engineering
Max-Planck-Institut für Eisenforschung GmbH
Max-Planck-Strasse 1, 40237 Düsseldorf (Germany)
E-mail: ikatsoun@illinois.edu
mayrhofer@mpie.de
Homepage: www.mpie.de/ecat

thus the electrochemical reaction rates.[12] However, the application of such catalysts under the conditions of the OER and the ORR faces severe challenges related to the activity, the stability, and the abundance of the materials used. In this Review, we focus on the recent developments regarding the understanding of the catalysis of the two crucial reactions, namely the OER and the ORR, in aqueous media from a surface electrochemistry point of view, and we describe the current and future challenges for designing materials that can be used for large-scale applications and extended operational times. For the important progress made in the field of molecular and enzymatic catalysis with regard to the water splitting and formation reactions, the interested reader is referred to other extended reviews.[13–15]

2. Fundamental Aspects of the Reactions of Interest

2.1. Thermodynamics

The equilibrium potential for the O_2/H_2O redox couple is given by the Nernst equation [Eq. (3)], where a_i is the activity of species i in water. The standard potential for the equilibrium shown in Equation (2) is $E^{o}_{O_2/H_2O} = +1.229\,V$ versus the standard hydrogen electrode (SHE), using the free energy for the formation of liquid water from oxygen under standard conditions.[16] Therefore, at 25 °C, the equilibrium potential becomes more negative by 59.2 mV versus the SHE for a one-unit increase in the pH value, and by 14.8 mV for a tenfold decrease of a_{O_2}, which equals the partial pressure of oxygen. In addition, the ORR and the OER may involve the formation of hydrogen peroxide as an intermediate [Eqs. (4) and (5)]. The corresponding equilibrium potentials are given by Equations (6) and (7), and the standard potentials for Equations (4) and (5) are $E^{o}_{O_2/H_2O_2} = +0.695\,V$ and $E^{o}_{H_2O_2/H_2O} = +1.763\,V$ versus the SHE, respectively.[17]

$$E_{O_2/H_2O} = E^{o}_{O_2/H_2O} - \frac{RT}{4F}\ln\frac{a^2_{H_2O}}{a_{O_2}a^4_{H^+}} \quad (3)$$

$$O_2 + 2H^+ + 2e^- \rightleftharpoons H_2O_2 \quad (4)$$

$$H_2O_2 + 2H^+ + 2e^- \rightleftharpoons 2H_2O \quad (5)$$

$$E_{O_2/H_2O_2} = E^{o}_{O_2/H_2O_2} - \frac{RT}{2F}\ln\frac{a_{H_2O_2}}{a_{O_2}a^2_{H^+}} \quad (6)$$

$$E_{H_2O_2/H_2O} = E^{o}_{H_2O_2/H_2O} - \frac{RT}{2F}\ln\frac{a^2_{H_2O}}{a_{H_2O_2}a^2_{H^+}} \quad (7)$$

2.2. Reaction Mechanism

The equilibrium in Equation (2) given above is an overall expression for the complete OER and ORR. However, both reactions involve several elementary steps, and in particular four electron-transfer steps, four proton-transfer steps (coupled or decoupled with the electron transfer), and one bond-breaking (ORR) or bond-forming (OER) step.[18] In this scenario, one additionally needs to consider that other processes, such as desorption/adsorption processes as well as chemical (e.g. disproportionation) reactions may occur and play an essential role in the product formation.[18] The above-mentioned steps always take place in series and lead to certain intermediates, and their sequence constitutes the reaction mechanism on a given surface. The elucidation of the mechanism of both reactions is important for the determination of rate-limiting steps; however, understanding the OER and ORR mechanisms is not easy due to the challenges of unambiguously interpretating kinetic data, identifying

Ioannis Katsounaros received his PhD on electrocatalysis from the Aristotle University of Thessaloniki with Dr. G. Kyriacou in 2009. Afterwards, he worked on the activity and stability of ORR catalysts at the Max-Planck-Institut für Eisenforschung. Since September 2013 he has been a Marie-Curie International Outgoing Fellow, working jointly at the Argonne National Laboratory and at the University of Illinois at Urbana-Champaign on energy conversion and storage.

Serhiy Cherevko studied physics at the V.N. Karazin Kharkiv National University (Ukraine) and received his MSc in 2004. He completed his PhD with Prof. C.-H. Chung in 2009 at the Sungkyunkwan University (SKKU; Republic of Korea), where he remained until 2011. Since then, he has been carrying out postdoctoral research at the Max-Planck-Institut für Eisenforschung. His research interests focus on processes at the metal(oxide)–electrolyte interface, particularly noble metal oxidation and dissolution.

Aleksandar R. Zeradjanin received his PhD in 2012 from the Ruhr-Universität Bochum, under the supervision of Prof. W. Schuhmann. Currently he is a research associate in the electrocatalysis group at the Max-Planck-Institut für Eisenforschung. His main research interests are in energy conversion at the electrochemical interface, including fundamental and applied aspects of electrocatalysis and electroanalytical chemistry.

Karl J. J. Mayrhofer received his PhD from the TU Vienna in 2006 after a research stay at the Lawrence Berkeley National Lab with Dr. N. M. Markovic. He then spent three years with Prof. M. Arenz at the TU München before becoming a group leader at the Max-Planck-Institut für Eisenforschung in the Department of Interface Chemistry and Surface Engineering. His research focuses on understanding the solid–liquid interface during electrochemical reactions and on the development of materials for energy conversion.

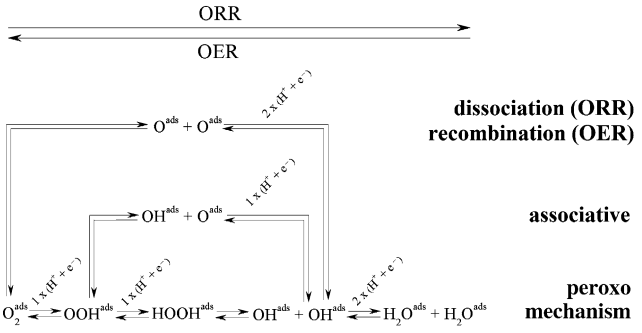

Scheme 1. Proposed ORR and OER mechanisms.

intermediates in situ (e.g. by spectroscopy), and explicitly supporting a preferable mechanism by means of electronic structure calculations when considering solvated systems.[19,20]

The proposed ORR and OER mechanisms can be unified in a single scheme (Scheme 1):

1) The ORR proceeds through a dissociation mechanism when the O–O bond of oxygen breaks directly upon adsorption and the formed O^{ads} is reduced successively to OH^{ads} and to H_2O^{ads}; reversing this mechanism yields the recombination mechanism of the OER.
2) The association mechanism for the ORR and the OER involves the formation of OOH^{ads}, which breaks into O^{ads} and OH^{ads} (for the ORR) or forms from the recombination of these species (for the OER).
3) Moreover, the ORR can proceed through the peroxo mechanism when two electron-transfer steps lead successively to OOH^{ads} and to $HOOH^{ads}$, and the latter then breaks into OH^{ads}; reversing this mechanism yields the peroxo mechanism for the OER.

2.3. Adsorption of Oxygenated Species on Transition-Metal Surfaces

The formation of adsorbed oxygenated species (e.g. O^{ads}, OH^{ads}, OOH^{ads}), originating from the aqueous electrolyte and/or the reaction itself, is considered as the decisive process for determining the catalyst performance. Oxidation of the surface can inhibit the ORR or enhance the OER, and may be involved in degradation processes, such as dissolution.[21,22] The adsorption energies of the oxygenated species involved in the ORR and OER mechanism on transition-metal surfaces and their oxides are proportional to each other.[23,24] This particular scaling relationship stems from a more universal correlation between the adsorption energies of any adsorbates bound similarly to a surface.[25,26] The existence of such a proportionality allows the adsorption energy of only one of the involved species (e.g. ΔE_O, ΔE_{OH}, or ΔE_{OOH}) to be considered when trying to determine catalytic trends. Moreover, the adsorption energy of a species on a transition-metal surface has been correlated to the position of the *d*-band center (ε_d) with respect to the Fermi level (ε_F) (known as the *d*-band center model).[27–29] According to this model, the metal–adsorbate (e.g. $M–O_{ads}$) bond is weaker when the distance between the Fermi level and the *d*-band center ($\varepsilon_F - \varepsilon_d$) is larger. Thus, the *d*-band center can be used (instead of the adsorption energy of a species on the surface) as an activity descriptor. Even though there are some reports that question if the *d*-band center alone is enough to describe the energy of adsorption,[30–32] this model still enables a simplified correlation, with good accuracy, between the catalytic activity and the surface electronic properties.

3. Catalysis of the Electrochemical Oxygen Reduction Reaction (ORR)

3.1. Activity for the ORR

3.1.1. Activity Trends for the ORR

The ORR is limited by either the formation of OOH^{ads} or the removal of OH^{ads}.[33] The existing scaling relations described in Section 2.3 impose a compromise between a neither too strong nor too weak binding of OOH^{ads} and OH^{ads} for the optimum ORR activity. This can be visualized by a volcano-type relationship (Figure 1) with respect to the

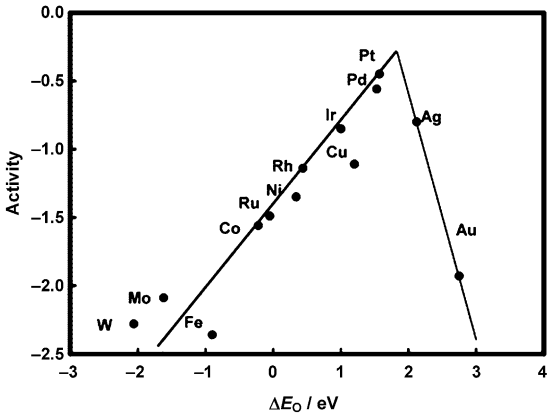

Figure 1. Volcano-type relationship for the ORR activity versus the oxygen binding energy. Reprinted from Ref. [34] with permission from the American Chemical Society.

adsorption energy of any oxygenated species, for example, the O_{ads}.[33,34] Catalysts located on the left side of the volcano in Figure 1 bind oxygen too strongly, and thus the reaction is retarded by desorption of the OH_{ads}. In contrast, for catalysts located on the right side of the volcano in Figure 1, the rate-determining step is the weak adsorption of oxygen as a reactant. The activity is maximized at the top of the volcano, and corresponds to a catalyst with a moderate binding energy of the oxygenated species.[33,34] However, the top of the volcano still does not correspond to a catalyst with a zero overpotential, because of the limitations that originate from the scaling relations.[35]

Of all the pure metals, platinum is the most active as it is located closest to the top of the volcano.[34] In the further discussion on noble metals for the ORR we will focus on Pt-based materials in acidic solutions, as they represent the most active and most studied systems.

3.1.2. Structural Sensitivity of the ORR—Size/Shape Effects

Even though the activation energy for the ORR in both acidic and alkaline media is about 40 kJ mol^{-1} on all single-crystalline Pt(*hkl*) surfaces,[36] different activities for the ORR have been measured. In particular, the activity for the ORR at +0.9 V versus the reversible hydrogen electrode (RHE) potential in 0.1 M $HClO_4$ decreases in the order 110 (4.2 mA cm^{-2}) > 111 (1.5 mA cm^{-2}) > 100 (0.34 mA cm^{-2}).[37] Moreover, different trends have been observed in H_2SO_4 (110 > 100 > 111) and KOH (111 > 110 > 100).[37–39] The structure sensitivity of the ORR has been attributed to the structure-sensitive adsorption of electrolyte species on Pt(*hkl*),[38,39] which act as "spectators" that influence the ORR activity without participating in the reaction itself. This structural sensitivity has been used to predict the effect of the particle size on the ORR, namely the decrease in activity with decreasing particle size, by considering that the ratio of terrace, edge, corner sites etc, depends on the geometry of a particle.[40–43] Following such geometrical considerations, the distribution of the surface sites changes rapidly for particles between 1 and 5 nm, thus leading to the strong adsorption of oxygenated species through an increased number of low-coordinated sites. This is expected to introduce a strong particle-size effect in this size range.[44–46] Apart from some ideal exceptions, where the particle size was controlled by layer-by-layer growth or by mass-selection of the platinum particles,[47,48] the experimentally derived trends in the decreasing activity on reducing the particle size do not match with the prediction from such models. In particular, little or no effect of the particle size has been observed with small (1–5 nm) high-surface-area particles, and the activity rapidly increases at larger particle sizes, until it reaches that of bulk platinum (Figure 2).[49–58] Moreover, the decreasing activity trends are the same regardless of the electrolyte ($HClO_4$, H_2SO_4, KOH; Figure 2),[56] which cannot be explained by the different activity trends between the Pt(*hkl*) surfaces in different electrolytes. Therefore, it seems that models that consider nanoparticles as ideal geometries with extended single-crystal facets are not sufficient to describe the particle-size effect for the more complex real nanoparticulate catalysts. This is probably because of effects related to the non-ideal shape of real catalysts, the mass transport of oxygen within micropores, the catalyst support, or the interparticle distance.[59]

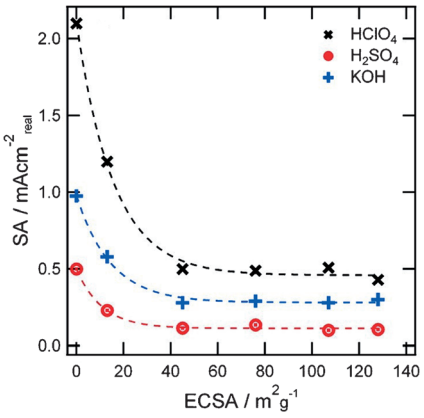

Figure 2. Area-normalized activity for the ORR versus the electrochemical surface area (ECSA), in three different electrolytes. Reprinted from Ref. [56] with permission from the American Chemical Society.

Nevertheless, various methods that enable the shape-controlled synthesis of nanostructures have been employed to prepare materials with a preferred orientation of surface sites, such as nanocubes, nanorods, and nanowires.[60–66] The shape-dependent ratio of crystallographic planes introduces differences in the activity for the ORR on platinum as well as on other metals.[67–70] In particular, by systematically imaging the ORR rates on various preferentially oriented nanoparticles by means of scanning electrochemical microscopy (SECM), it was shown that the ORR activity decreases in the series hexagonal > tetrahedral/octahedral ≈ spherical > cubic nanoparticles in 0.1 M $HClO_4$ solution, while the order changes to hexagonal > cubic > spherical > tetrahedral/octahedral nanoparticles in 0.5 M H_2SO_4.[68]

3.1.3. Alloying Pt with Transition Metals

To optimize the activity of Pt for the ORR and come closer to the top of the volcano (Figure 1), the adsorption energy for oxygen should be lowered by approximately 0.2 eV.[71] This can be achieved by alloying platinum with certain transition metals, such as Cu, Co, or Ni. These alloying components induce 1) a "ligand effect", which originates from bonding interactions between the active platinum atoms on the surface and the alloying metal atoms in the second or third layer, and 2) a "strain effect", which originates from the compressed arrangement of platinum atoms on the surface because of disturbances imposed by the shorter interatomic distance of the alloying metal atoms that are located underneath.[72] Although it is not straightforward to distinguish between the relative contribution of the two effects, as they typically occur in parallel, it is clear that they both result in a modification of the surface electronic properties of the platinum and thus in different chemisorption properties.[72] On the basis of the *d*-band center model, the specific alloying leads to a downward shift of the *d*-band center with respect to the Fermi level, and thus to a weakening of the Pt–O bond.[29,71,73]

The resulting enhanced activity for the ORR has been demonstrated on bulk Pt alloys, and also for specific bimetallic surfaces, prepared by different synthesis procedures:

1) the "platinum monolayer" approach,[74–77] where a platinum monolayer is deposited on a non-platinum metal substrate (e.g. palladium) by galvanic replacement of a metal (e.g. copper) adlayer that has been obtained by underpotential deposition;
2) the "platinum skin" approach,[73,78,79] where segregation of a pure Pt atomic layer on top of an alloying metal-rich second layer is induced by thermal annealing, and
3) the more recent "near-surface-alloy" approach,[80–82] where a metal (e.g. copper) adlayer obtained by underpotential deposition on platinum is exchanged upon annealing with the platinum atoms directly beneath, thereby leading to a thin platinum monolayer on top of

the second layer that consists mainly of foreign metal atoms.

Regardless of the preparation method, volcano-type relationships between the oxygen adsorption energy (or the *d*-band center) and the ORR activity for various alloys have been derived experimentally.[73,75,80]

Extensive efforts have been directed over the last few years towards the preparation of applied bimetallic nanostructured electrocatalysts with an enhanced activity for the ORR.[83–89] Nanoparticles based on alloying platinum with transition metals, approximately in a stoichiometry of Pt_3M (M: Cu, Co, Ni, ….) are generally more active than pure platinum particles, and the activity follows the same trends as those established for model surfaces.[50,89–95] However, the activity enhancement on alloy nanoparticles is typically slightly lower than that on extended surfaces, so it is of major importance to control the size, shape, and initial alloy composition of nanoparticles upon synthesis, as they all have an important impact on the catalyst performance.[96–100] Hence, the morphology of pure platinum and platinum-alloy nanoparticles must be about the same when quantifying the impact of the second metal on the activity for the ORR.[101] A remarkably high activity for the ORR was observed on so-called core–shell nanoparticles, formed typically by nanoparticles with an originally high alloying metal content, PtM_3 (Figure 3). Removal of the alloying metal from the top layers by electrochemical dealloying yields particles that consist of a Pt-enriched shell of a few layers and a PtM_3 core.[96,102–108] Depending on the size of the particle, the inner part may consist not only of a single core, but also of multiple, irregularly shaped cores, which may even exhibit some porosity with very large particles.[109,110] As a result of the excessive leaching of the alloying component from the top layers in the electrochemical environment, the strain effect has been used to explain the high activity of such bimetallic catalysts. It should be noted, however, that it still remains an open question as to what extent the presence of the alloying metal atoms several layers under the topmost platinum atoms can contribute to an increased ORR activity.[111]

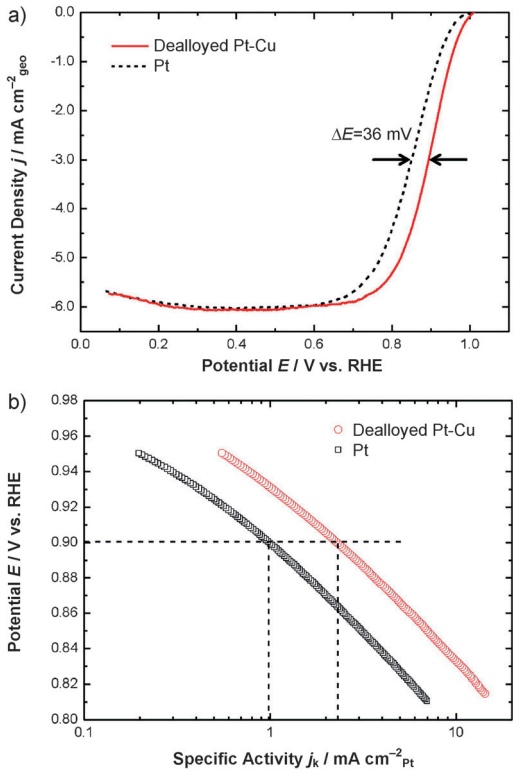

Figure 3. a) Hydrodynamic voltammograms (1600 rpm) for the ORR on dealloyed $PtCu_3$ and pure Pt sputtered thin films, recorded in O_2-saturated 0.1 M $HClO_4$ solution at room temperature (scan rate: 20 mV s^{-1}). The arrows indicate the values of half-wave potentials. b) Tafel plots for the dealloyed $PtCu_3$ and pure Pt films, indicating the activity enhancement at +0.9 V_{RHE}. Reprinted from Ref. [108] with permission from the American Chemical Society.

3.2. Stability of the Platinum-Based ORR Catalysts

Considering that the prospect for a further significant enhancement in the ORR activity is probably limited, the long-term performance of fuel cells has become the most important challenge that currently needs to be addressed.[112] To compete with conventional internal combustion engines, a fuel cell should maintain at least 90% of its performance after 5000 h of operation (equivalent to 250000 kilometers), including thousands of start-up and shut-down events.[113] The lifetime of the fuel cells is limited by several factors, which are all interrelated and may act synergistically; for a discussion on the important impact of such factors to the overall fuel-cell durability the interested reader is referred to previous reviews on this topic.[114] In this Review, we will focus entirely on the stability of the nanostructured catalyst itself, which can undergo severe degradation during operation (particularly during fuel-cell start-up and shut-down), which leads to a decrease in the active surface area and an increase in the ORR overpotential. The mechanisms described in Section 3.2 and are responsible for the degradation of carbon-supported Pt-based catalysts, may occur in parallel during operation, as

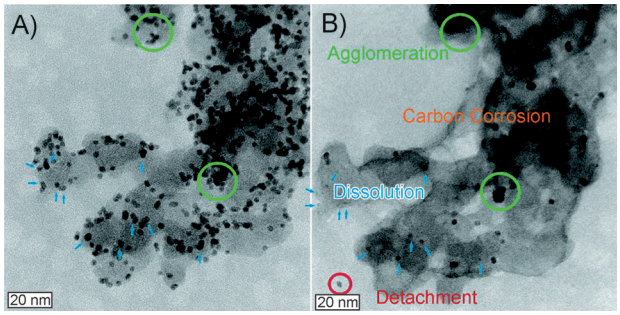

Figure 4. Comparison of the same catalyst location A) before and B) after electrochemical treatment (3600 cycles between +0.4 and +1.4 V_{RHE}, 1 V s^{-1}). Four degradation mechanisms occurring in parallel on a commercial Pt/C catalyst are shown: dissolution (blue), support corrosion (orange), agglomeration (green), and detachment (red). Reprinted from Ref. [115] with permission from the American Chemical Society.

can be visualized (Figure 4) using identical location transmission electron microscopy (IL-TEM).[115] This overlap of mechanisms highlights the inherent difficulty in understanding and preventing the loss of active surface area that is observed macroscopically.[116]

3.2.1. Platinum Dissolution

The dissolution of platinum is a fundamental process that can occur on any (nanoparticulate or extended) platinum surface. Smaller particles are more susceptible to dissolution due to their higher surface energy (Gibbs–Thomson effect).[117,118] Individual platinum particles that dissolve become reduced in size, which has been visualized directly (Figure 4).[115,119] Within a fuel cell, platinum dissolution from nanoparticle catalysts may result in: 1) removal of platinum with the water outlet stream,[120] 2) redeposition of platinum on larger particles, that is, Ostwald ripening,[121,122] and 3) reduction of dissolved platinum with permeated hydrogen and redeposition within the membrane.[123,124] It is well-established that Pt dissolution is more pronounced during potential cycling than under steady-state conditions,[21,125–127] although there has been no consensus on whether platinum dissolves during the positive- or the negative-going sweep.[125,127–132] Recently, it was possible to unambiguously distinguish between an anodic and a cathodic dissolution process, with the latter being more prominent by far, particularly through the increase in the upper potential limit.[21] This confirms previous assumptions that platinum dissolution is associated with changes in the Pt state (e.g. from the oxidized to the reduced Pt state or the opposite).[132–134] Even though the exact mechanism of the dissolution of platinum still remains unclear, a certain interrelation between Pt dissolution and Pt-O site exchange at high potentials and leading to weakly bound platinum species is likely the cause, as such species are more susceptible to dissolution.[132,135–137]

Further investigations need to be directed to an overall understanding of the dissolution of other noble metals[22,138] and their alloys,[139] as well as of applied catalysts, which will inspire extensions of theoretical models and enable the prediction and prevention of the dissolution of nanoparticle catalysts in applied systems under various operating conditions.[133,134,140–142]

3.2.2. Ostwald Ripening

Following the dissolution of platinum from small particles, the redeposition of dissolved platinum species on larger particles may occur as a consequence of the reduction of the surface energy. During Ostwald ripening, small particles shrink, while large particles become even larger; therefore, an overall increase in the average particle size is expected. One can distinguish between two types of Ostwald ripening: 1) a 3D process, when dissolved species are transported through the electrolyte prior to reduction and deposition,[122] and 2) a 2D process when dissolved platinum is transported on to the carbon support prior to deposition.[121] Direct visualization of Ostwald ripening occurring in thick catalytic films under harsh potential cycling conditions was recently achieved.[143]

3.2.3. Corrosion of the Support

The oxidation of carbon to CO_2, which is thermodynamically possible above $+0.207\ V_{RHE}$,[144] is kinetically limited below $+1.2\ V_{RHE}$ depending on the temperature.[145] On the basis of early gas phase oxidation studies,[146] it has been proposed that the corrosion of high-surface-area carbon is initiated by the corrosion of disordered carbon sites in the core of the carbon particles.[147,148] Such degradation, which occurs at elevated temperatures and leads to a hollow-like or a shrinked structure, was recently visualized in electrochemical studies.[149] At room temperature, severe carbon corrosion leading to a shrinkage of the support structure and even to a complete removal of a whole fraction of the aggregate has been observed under harsh potential conditions (see also Figure 4).[115,150]

Carbon corrosion has important consequences, as it can accelerate secondary degradation mechanisms such as agglomeration and particle detachment,[115] while the associated loss of porosity can severely limit the mass transport of reactants and thus deteriorate the performance in the electrochemical reactor.[151]

A variety of other carbon supports has been developed to overcome these issues,[152] such as multiwalled carbon nanotubes,[153,154] graphene,[155] ordered mesoporous or nanoporous carbons,[156,157] hollow graphitic spheres,[158] activated carbon nanofibers,[159] and carbon aerogels.[160] In some cases, the durability of the catalyst was superior to conventional nanostructures; however, a deep understanding of the impact of the support morphology on retarding individual degradation mechanisms is still lacking. An alternative strategy to address the stability issues of carbon-based materials is to use transition-metal oxides as supports. Typically, so-called Magnéli phases (Ti_nO_{2n-1}, on average Ti_4O_7), but also WO_3, NbO_2, TaO_2, and TiO_2 have been employed because of their remarkable stability under fuel-cell conditions, low cost, commercial availability, ease of control of the size and structure, and good dispersion of the catalyst.[161–163] However, such oxides typically have low electronic conductivity, which has to be increased by producing oxygen vacancies or introducing an appropriate dopant. In addition, the use of unsupported platinum nanostructures has also been investigated as a way to avoid the contribution of support corrosion in the overall degradation.[62–64,70] A different, prominent approach was pioneered by 3M, with the so-called nanostructured thin-film (NSTF) catalysts, which consist of platinum sputtered onto oriented arrays of crystalline organic-pigment whiskers.[164,165] These catalysts are not only more active than carbon-supported catalysts, almost matching the specific activity of extended surfaces, but they are also significantly more resistant to primary degradation mechanisms.

3.2.4. Agglomeration

The agglomeration of platinum particles leads to particle growth and thus to decreased utilization of platinum with respect to its mass. Agglomeration occurs when smaller particles come in contact and form a larger particle (Figure 4),

in a reshaping process that is driven by the reduction of the surface energy.[149] Particles may originally be in contact after synthesis; in that case they may immediately coalesce, depending on the potential. Otherwise, contact has to be established in the following ways prior to coalescence:[115,116,166] 1) adjacent particles may approach each other as a result of the shrinkage of the support following carbon corrosion (see Section 3.2.3) 2) particles may migrate over the support and come into contact with other adjacent particles, which may also show some mobility. The probability of agglomeration is inversely dependent on the interparticle distance;[167] thus, the probability increases at areas with high particle density,[115,168] or in cases of higher platinum content.[169]

3.2.5. *Particle Detachment*

The complete loss of platinum particles that detach from the support, thereby leading to a decrease in the total number of particles without introducing a change in the particle size, is an additional mechanism that has been visualized by electron microscopy (Figure 4).[115,149,170–172] Particle detachment originates from a weakening of the particle–support interaction,[173] and can thus be initiated by corrosion of the support.[149] For this reason, detachment and agglomeration are usually observed in parallel, as both can occur after carbon corrosion.[115,149,168,172]

3.2.6. *Leaching of Alloying Metal Atoms*

The less-noble metal atoms typically suffer from selective dissolution during operation of the fuel cell, even in already preleached alloys, which leads to a gradual loss of the enhancing effect of the alloying metal on the ORR activity (Figure 5).[166,174,175] Depending on the initial composition and size, the remaining particles can form porous structures or thicker Pt-enriched shells. Moreover, the dissolved less-noble metal can cause additional issues for the overall performance of the fuel cell. The exchange of protonic sites in the ionomer with metal cations can lead to[50,120,176] 1) higher resistance of the membrane and the catalyst-layer ionomer, 2) lower oxygen diffusion in the ionomer, and 3) degradation of the membrane through the formation of peroxo radicals. In addition, the dissolved metal ions may migrate across the membrane and deposit on the anode of the fuel cell.[110]

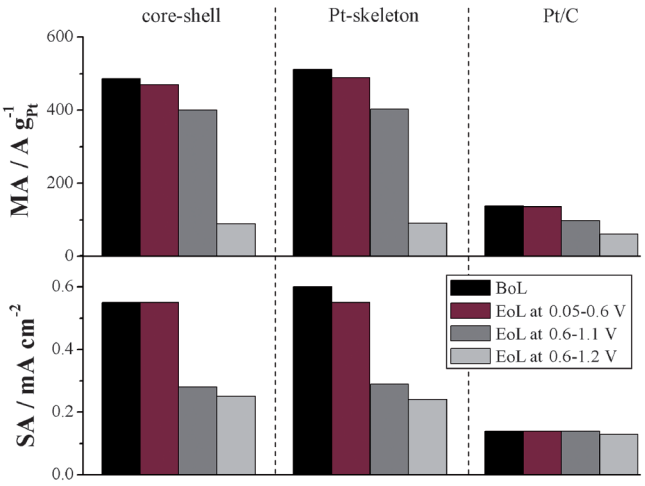

Figure 5. Specific and mass activities of the Pt_3Cu/C core–shell, Pt_3Cu/C skeleton, and
Pt/C catalyst at the beginning (BoL) and end of life (EoL), namely before and after 10000 degradation cycles in 0.5 M H_2SO_4 in the potential window indicated in the legend. The activities were measured at 0.9 V_{RHE} in the same electrolyte. The Figure was constructed from the data published in Table 1 of Ref. [183].

In an acidic environment, the dissolution of the non-noble metal surface atoms (such as Cu, Co, etc) is thermodynamically favorable at potentials to which the ORR catalysts are exposed, but alloy material in the core underneath a Pt shell is also susceptible to dissolution. Three mechanisms, which may occur in parallel, can be considered as possible explanations of these observations:

1) the diffusion of platinum surface atoms may not allow the formation of a uniform protective layer of Pt, thus leaving some alloying metal atoms exposed to the electrolyte,[177]
2) the alloying metal atoms can segregate to the surface,[178,179] and
3) dissolution of the alloying metal atoms can follow the dissolution of platinum atoms in the protective shell.[21]

In any case, the dissolution of the less-noble metal may continue, possibly until only platinum atoms remain in the nanostructure. Of the various platinum alloys that have been investigated, extended Pt_3Y and Pt_5Gd surfaces seem to be the most stable.[180–182] However, the preparation of the corresponding nanoparticles is not straightforward because the standard potentials for the Y^{3+}/Y and the Gd^{3+}/Gd redox couples are very negative.

3.3. *Abundance of the Materials Used in ORR Catalysts*

If all the platinum produced annually (ca. 200 t yr^{-1})[184] was used for hydrogen/air fuel cells at state-of-the-art loadings, it would only suffice for approximately 4–5 million cars per year. As a consequence of the limited availability of platinum and the related high cost, massive efforts have been directed toward the synthesis of ORR catalysts based on more abundant (and cheaper) non-noble materials.[185] The main challenge in this case is to design catalysts that will at least approach the activity of platinum, but at the same time will be stable for long-term operation under acidic conditions. In alkaline media, non-noble materials typically exhibit a lower overpotential for the ORR and better stability compared to acidic electrolytes.[186] A highly inspiring letter to *Nature*[187] in 1964 motivated extensive research toward the synthesis of pyrolyzed transition-metal-containing macrocyclic compounds, such as metal phthalocyanines and metal porphyrins.[188–191] More than two decades later it was shown that the complex macrocycles can be replaced by other nitrogen-containing polymers capable of binding transition metals,[192] thereby highlighting the essential role of the transition-metal ion coordinated by nitrogen atoms (MeN_xC_y) in the observed catalytic activity. Some authors have proposed that the metal ion does not remain in the active site after the heat treatment,

but only catalyzes the formation of the active sites consisting of only nitrogen and carbon during the heat treatment, thus leading to the so-called "metal-free catalysts" after chemical leaching.[193–196] However, there is as yet no undisputed evidence that the chemical leaching can entirely remove the metal from the heat-treated catalyst. Instead, it has been shown that the ORR on Fe/N/C is inhibited by the presence of iron-complexing cyanide, thus indicating the existence of a metal-based active site for the ORR.[197]

Following the notion that a high density of active MeN_4 sites per unit volume is required to create active non-noble metal catalysts, intensive efforts have been made over the last few years to develop novel synthesis routes.[198–207] In addition, a lot of work has been carried out to resolve the mechanism of the ORR on non-noble metal catalysts, as well as the nature of the active sites.[197,208–212] These studies have led to significant improvements and breakthroughs in the activity of non-noble catalysts for the ORR, which can almost approach the activities obtained on platinum;[200,201] excellent reviews have recently been published.[213,214] In one of the prominent examples, remarkably high activities (Figure 6) were obtained

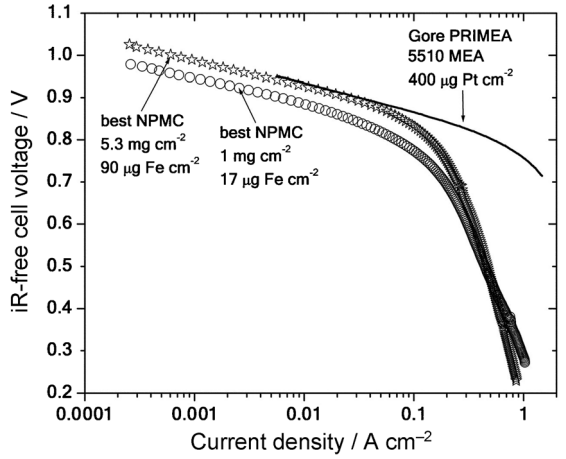

Figure 6. Voltage–current curves in a H_2/O_2 fuel cell using membrane electrode assemblies (MEAs) with a cathode made of two loadings of the best nonprecious-metal Fe/N/C catalyst (NPMC) synthesized by Lefévre et al. Also shown is the comparison with a commercial Gore PRIMEA 5510 MEA (W. L. Gore & Associates) with 0.4 $mg_{Pt}\,cm^{-2}$ loading at the cathode. Reprinted from Ref. [200] with permission from AAAS.

by synthesizing catalysts consisting of nitrogen-coordinated iron incorporated into microporous carbon.[200] The authors attributed the observed high catalytic activity to the formation of a high density of Fe-N_4 sites within the micropores of the carbon support. To approach the performance of commercial Pt/C catalysts (0.4 $mg_{Pt}\,cm^{-2}$) in the fuel cell, loadings in the order of a few $mg\,cm^{-2}$ were required, which results in a high catalyst layer thickness. This has the consequence that severe mass-transport limitations on the cathode can occur in a H_2/O_2 and—even more so—in a H_2/air fuel cell, thereby leading to drops in performance at high current densities (Figure 6). Despite the major advances in regard to activity, the largest challenge, namely the stability of non-noble materials at operating temperatures, will have to be addressed more intensively in the future to render such a material class viable for applications. The stability issues that the non-noble materials experience are related to the oxidation of transition-metal-based active sites by the intermediate H_2O_2, oxidation of the carbon support, and exposure of the cathode to high potentials. An excellent description of these issues for non-noble materials is provided in a recent review.[213]

4. Catalysis of the Electrochemical Oxygen Evolution Reaction (OER)

4.1. Activity for the OER

4.1.1. Activity Trends for the OER

In contrast to the ORR, the oxygen evolution reaction always proceeds on oxidized surfaces,[215–217] and is limited either by the strong adsorption of OOH^{ads} or the weak adsorption of O^{ads}.[218] Based on the existing scaling relations that were described in Section 2.3, the difference in the free binding energy between O* and OH* was introduced as a universal catalytic descriptor for the OER to construct volcano-type plots (Figure 7a).[24] According to the Sabatier principle, an optimal, moderate binding energy of the OER intermediates assures the highest catalytic activity.[219] The obtained theoretical activity trends are, in general, consistent with old experimental investigations, which showed that the activity toward the OER on rutile-, spinel-, or perovskite-type oxides follows a volcano-type dependence on the enthalpy change of the transition from a lower to higher oxide or other similar activity descriptors.[24,220–222] Thus, a good correlation between the theoretical and the experimental overpotential toward the OER was observed (Figure 7b).[24] Experimentally, rutile-type RuO_2 was found to exhibit the highest activity for the OER (Figure 8).[220,223,224] Compared to a theoretical optimum catalyst, the oxygen adsorption on RuO_2 is slightly too weak.[218]

Despite the general aggreement between theory and experiment, some discrepancies still exist; for example, according to DFT calculations Co_3O_4 should exhibit a slightly lower overpotential than even RuO_2 (Figure 7a).[24] Such discrepancies between theory and experiment may derive from the simplification made when using a single activity descriptor, and/or from the fact that the model surfaces that are used for computational predictions do not completely capture all the characteristics of polycrystalline surfaces, such as of surface defects and of changes in the surface state occurring during the reaction.

Since alkaline electrolyzers operate at current densities that are about 2–3 times lower than that of acidic electrolyzers,[225,226] we will focus in the next subsections, as for the ORR, mainly on nanostructured electrocatalysts for the OER in an acidic environment.

4.1.2. Structural Sensitivity of the OER

To understand the relationship between structure and activity toward the OER, it would be desirable to distinguish

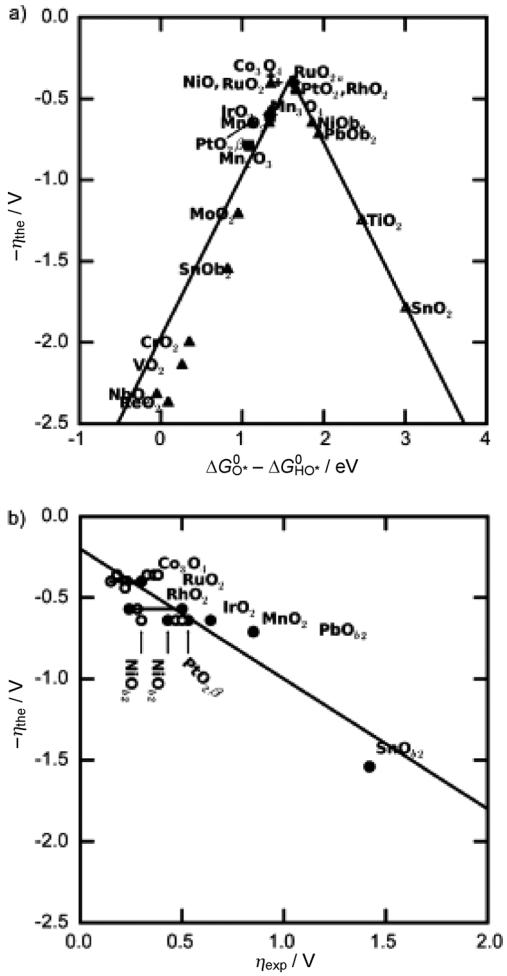

Figure 7. a) Theoretical overpotentials for the OER on various oxides, versus the difference in the free binding energy between O* and OH*. b) Theoretical overpotential versus the experimental overpotential in acidic (filled squares) and in alkaline media (empty circles). Reprinted from Ref. [24] with permission from Wiley.

between electronic and geometric effects by analysis of well-characterized model surfaces, such as single crystals,[227] as for the ORR. However, the interpretation of single-crystal data for the case of the OER is not trivial, because the reaction proceeds on surfaces, which typically undergo reconstruction upon the formation of surface oxide and evolution of oxygen. Thus, the observations may not directly reflect the nominal model structure. However, some structural sensitivity has been observed, for example, for the case of gold single crystals in the low current density region close to the onset of the OER, where the activity increases in the order Au(110) > Au(111) > Au(100).[217] Interestingly, a comparison of different RuO_2 surfaces revealed that the Tafel slopes for all single-crystal surfaces is higher than for polycrystalline RuO_2.[223,227] This may imply that the activity of the polycrystalline RuO_2 toward the OER is not simply an average property of individual single-crystal components.

The utilization of active nanostructures is also necessary to obtain high surface areas and a limited content of noble-metal-based oxides for the OER. In general, the activity trends for nanoparticulate catalysts are the same as those observed for bulk materials (Figure 8) and predicted from theory.[224,228] One of the most intriguing phenomena in the description of the OER is the influence of the particle size on the catalytic performance, however, in contrast to the ORR, there are only a few systematic studies dealing with the effect of the particle size on the OER. The Tafel slope is independent of the particle size with small particles, but above a critical size the Tafel slope increases rapidly with increasing particle size.[229] Moreover, the activity for the OER decreases with an increase of the size of RuO_2 particles in the region from 15 to 45 nm (Figure 9).[230,231] This trend was also confirmed for smaller particles.[232] This dependence of the activity on the particle size implies that crystal edges, which are widely present in smaller particles, play an important role in the catalysis of the OER on RuO_2 by being preferential reaction sites for the OER.[233] Similarly, the OER activity decreases with the increase in the size of

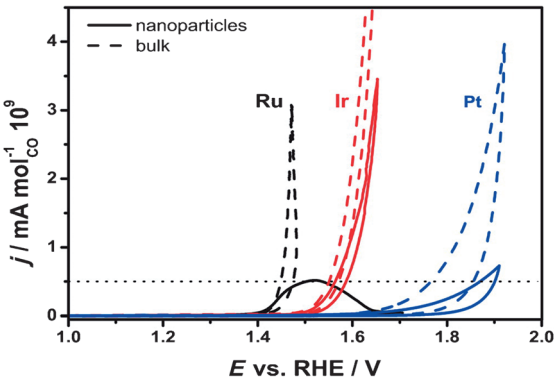

Figure 8. Hydrodynamic voltammograms (1600 rpm) recorded on bulk and nanoparticulate Ru, Ir, and Pt with 6 mVs^{-1} in N_2-saturated 0.1 M $HClO_4$ at room temperature. The curves represent the first cycle recorded. The current was normalized to the number of surface sites determined from CO-stripping experiments. Reprinted from Ref. [224] with permission from the American Chemical Society.

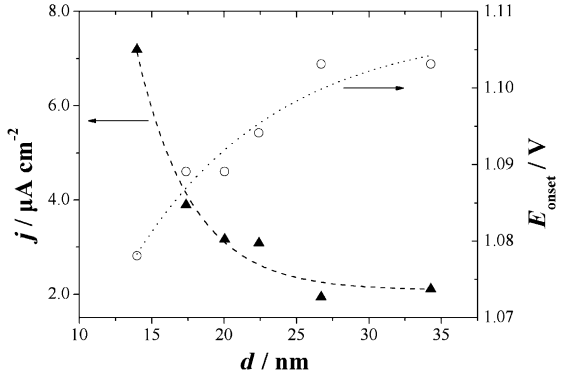

Figure 9. Activity (left *y*-axis) and onset potential (right *y*-axis) for the OER versus the diameter of the RuO_2 particles in 0.1 M $HClO_4$. The activity was determined at +1.20 V versus SCE in this electrolyte after normalization to the real surface area. The onset potential is expressed versus the same reference. The curves are drawn as a guide to the eye. The Figure was constructed from the data published in Figure 5 of Ref. [231].

IrO_2 particles.[234] In contrast, Co-doped RuO_2 exhibits an opposite behavior,[230] which indicates that the crystal edges do not play an important role on the kinetics of the OER in this case. This may be attributed to a different rate-determining process for the two materials; in particular, it was suggested that the OER is controlled by charge transfer on RuO_2, while on Co-doped RuO_2 the rate-determining step is the recombination of the oxygen at the electrode surface.[230] The support has an effect on the catalytic activity of nanosized particles, which can be attributed to a better utilization of the active sites and/or to interactions between the catalyst and the support.[163,235,236] In addition, the spatial distribution of the active sites and prevention of surface segregation is of high importance for the performance of gas-evolving electrodes.[237–239] Thus, direct monitoring of the local activity for the OER at the solid–liquid interface becomes necessary to study certain nanostructural effects clearly.[240,241]

4.1.3. Importance of the Void Fraction in Nanostructured Catalysts for the OER

One distinct feature which separates the gas-consuming ORR and the gas-evolving OER on high-surface-area catalytic layers is that the OER proceeds with an increase in overpressure across the electrode–electrolyte interface.[242] This means that reaction sites in the "inner" surface also become active with an increasing overpotential and means the reaction "spreads" into the inner catalytic layers.[243] This is opposite to the ORR, where only the outer surface atoms are active when the reduction becomes diffusion-limited upon increasing the overpotential. In this sense, it is of major importance for the OER to also consider the void fraction or porosity of the catalytic layers during synthesis. A very promising approach for catalyst design in heterogeneous catalysis is the preparation of a system with trimodal pore porosity.[244] Particularly the macro- (pore size >50 nm) and the mesoporosity play an essential role, as the microporous fraction (pore size <2 nm) of the total surface is relatively inaccessible by reactants during electrochemical reactions. The mass transport of species inside the micropores may be orders of magnitude lower than in the bulk solution.[245,246]

Another essential part of the hierarchical architecturing of catalytic layers for the OER is structuring for the efficient detachment of gas bubbles. Namely, the availability of active sites and thus the efficiency of gas evolution strongly depend on the surface morphology. When the rate of the OER becomes sufficiently high, the concentration of oxygen at the solid–liquid interface may overcome the saturation concentration expected from Henry's law, so that not all the O_2 molecules produced can be completely solvated.[247,248] Gas bubbles start to form and behave like a "sink" for further dissolved gas.[249] The gas phase at the solid–liquid interface, however, can block parts of the electroactive surface area, which causes an inhibition of the macrokinetics of the electrode (increase in overpotential).[250] A minimization of the gas-bubble detachment radius can significantly increase the frequency of gas-bubble detachment. A key strategy in performance optimization is, thus, the introduction of pores, cracks, and/or channels into the electrode structure, where nucleated gas bubbles are limited in growth.[251] Efficient catalyst morphologies can promote the detachment of small bubbles with a high frequency, which was confirmed experimentally using SECM.[252] The acceleration of gas evolution was already also shown to be a very promising strategy for decreasing the overpotential for similar reactions, such as chlorine evolution.[251,253,254]

4.1.4. Mixed Transition-Metal Oxides

Analogous to alloying Pt with transition metals in the case of the ORR, various mixed metal oxides are commonly employed instead of pure RuO_2 or IrO_2 as catalysts for the OER.[255] The aim is to 1) tune the intrinsic OER activity,[241] 2) stabilize the catalytic component,[256] and 3) reduce the noble-metal content.[257] Increased activities compared to RuO_2 can, for example, be achieved with a TiO_2/RuO_2 mixed oxide.[241] This enhancement was attributed to the promoted charge transfer from RuO_x towards TiO_2, which fits into the general expectation that charge transfer on surfaces that contain mixtures of two transition metals will occur to the element with the larger fraction of empty states in its valence band.[258] Another very promising coating with remarkable activity and stability is Ta_2O_5/IrO_2,[259] where the catalytically active component IrO_2 in a tetragonal rutile-type structure is incorporated into a Ta_2O_5 matrix. In such structures, the amount of active and expensive Ir can be reduced by the addition of Pd, Nb, etc, while still maintaining the original activity.[260–262] Moreover, an increase in the activity can be achieved by mixing Ir with Ru.[256,263] The properties of all these oxide layers depend strongly on the preparation method.[264] An usual approach to obtain mixed metal oxide catalysts for the OER is based on the thermal decomposition of mixtures of solutions of precursor salts.[265] Another common synthesis route is the sol–gel procedure.[266] Regardless of which preparation method is followed in the synthesis, the precursor employed has a pronounced influence on the physicochemical properties and the performance of the catalytic layer.[267] During the synthesis of mixed-metal oxides, the effective conversion of the precursor salt, the crystallization, and the formation of the active rutile phase depend strongly on the thermal treatment. The proper choice of synthesis temperature is additionally important to avoid decomposition of the metastable solid solution into individual oxides on the surface, and to prevent the formation of an insulating layer between the support and the catalytic layer.[253] Certainly, to form mixed oxides in the form of a solid solution, it is important that the parameters of the crystal lattice match according to Hume–Rothery rules.[268] Furthermore, if the loading of the noble component needs to be reduced, limitations arising from percolation phenomena may be introduced. The possibility of obtaining randomly distributed isolated clusters increases particularly for very low loading. In that case, the clusters, even though they are catalytically active, can be electrically disconnected from the support and, thus, not contribute to the reaction.[269]

4.2. Stability of the OER Catalysts

Substantial progress has been made over the last few decades in terms of the synthesis and characterization of different catalysts for the OER, with the focus typically placed on enhancing the slow kinetics of the reaction, as described in Section 4.1.[224,228,270–275] In contrast, stability issues, which constitute an essential part of the catalyst performance, have been investigated to a more limited extent.[276–282] The OER catalysts may undergo severe degradation under the demanding technical conditions of the OER (Figure 10). In acidic media, oxides with rutile-type structures

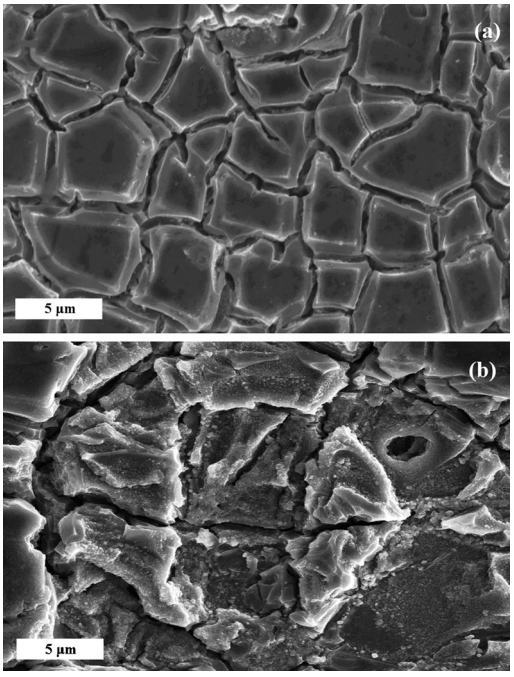

Figure 10. Scanning electron microscopy images of an oxygen-evolving RuO_2 anode catalyst supported on Ti a) before and b) after electrolysis for 1 h in 1 mol L^{-1} H_2SO_4 at a current density of 10 kA m^{-2}.

are typically the most promising in terms of long-term stability, while in alkaline media, perovskite- and spinel-type oxides were additionally suggested for the OER under technical conditions.[221,223]

One general problem of (electro)catalysis that arises is finding appropriate stability descriptors, which would help to understand relationships between structure and stability and predict the long-term performance of the catalyst.[283] The notion introduced by Bockris and Otagawa[221] that the more active catalysts for the OER will simultaneously suffer from low resistance toward corrosion is oversimplified, although it will certainly be very hard to decouple the stability of active sites from actual turnover per active site. Given the difficulty of finding appropriate stability descriptors for the wide range of material classes, different combinatorial approaches can be followed to study the stability of material libraries.[284–287]

The standard catalysts for the OER are based on so-called dimensionally stable anodes (DSAs),[288] which consist of a coating active for the OER deposited on a base metal.[289,290] DSAs are usually synthesized by co-precipitation of transition-metal oxides with oxides of titanium or other transition metals. In contrast to the weak van der Waals interaction between nanoparticles and a high-surface-area carbon support on which they are dispersed, the nanostructured catalytic layers with hierarchical porosity and crystalline structure are strongly linked with the Ti support through chemical bonds.[237] Therefore, they exhibit not only remarkable chemical and electrochemical, but also notable mechanical stability. Detailed information about the DSAs can be found in an excellent review.[291] Despite their remarkable stability, DSAs still suffer from certain degradation mechanisms under the extreme OER conditions.[276,291]

Alternatively, carbon-supported nanostructures have been frequently used for the electrocatalysis of the OER.[284,285,292,293] As described in Section 3.2.3, carbon can already undergo corrosion at sufficiently positive potentials (above $+1.2\,V_{RHE}$) at room temperature, which makes carbon rather unsuitable as a support for OER catalysts. Even the more stable graphitic materials have to be replaced in cases when OER is only a side reaction, for example during the evolution of acidic chlorine.[291] Additionally, the utilization of unsupported catalysts directly sprayed on the membrane was also reported as a way to improve the catalyst stability.[282,294]

4.2.1. Degradation of the Support

During the OER, the electrolyte can penetrate through the porous coating toward the Ti support, and the oxidation of water can lead to TiO_x growth at the interface between the metallic support and the catalytic layer. After the nucleation of the oxide at preferential sites, the oxide grows further laterally, thereby leading to a decrease in the conductive area at the support–catalyst interface. To maintain the same current density when operating under galvanostatic conditions: 1) the electrolyzer voltage increases, thereby leading to higher energy consumption, and 2) the local current densities at areas which are not yet covered by TiO_x increase, so that the TiO_x growth is also accelerated in these areas until the entire support–catalyst layer is covered by the insulating TiO_x oxide. Experimental evidence of the appearance of the passivating oxide layer has been obtained by using various methods,[237,295] and detailed explanations about the oxide growth mechanism are provided elsewhere.[296–298] A conducting and protective intermediate layer between the Ti support and the catalytic layer can be introduced, for example, to prevent such a passivation of the support.[299]

In the case of impure electrolytes, the degradation of the support can, however, also be dominated by dissolution of the base metal.[276] If the electrolyte penetrates through the porous catalyst coating towards the support (Ti), only a few ppm of fluoride ions are sufficient to attack the titanium. Fluoride ions can form various soluble complexes with Ti through chemical reactions, independent of the polarization of the electrode. This occurs even when titanium is partially passivated. Eliminating fluoride ions from the electrolyte in a membrane reactor remains critical, even though some approaches, for example, based on using Ca^{2+} or Al^{3+} as

complexing agents, have been proposed.[276] Besides Ti, the degradation of other base metals, such as Ta and Sn, is also of interest; Ta is much more stable towards corrosion, although it is very sensitive to oxidation at elevated temperatures.[300]

4.2.2. Dissolution of the Catalyst Layer

Efficient electron transfer during the OER on various oxides is related to redox transitions with standard potentials in the range of those of the reaction.[301,302] For example, the onset for the OER on RuO_2 coincides with the transition of the oxide from a lower (e.g. RuO_2) to a higher (RuO_4) oxidation state ($E^o = +1.387\ V_{NHE}$ for Ru^{2+}/Ru^{4+}). Following this transition, the oxide in the higher oxidation state, which is an actual intermediate of the OER, will be reduced again to the initial state by accepting electrons from the oxygen-containing species of deprotonated water (O*, OH*, …). Although the activity of RuO_2 depends on the potential of the RuO_4 formation, the stability depends on the solubility of RuO_4.[276,303,304] Similarly, dissolution has been observed during the OER on IrO_2, where soluble IrO^{4+} species are formed at potentials above $+2.0\ V_{SHE}$.[270] This potential is, however, significantly higher than that reached at practical current densities, so that the dissolved amounts are rather low. The dissolution of Ir was suggested to occur at potentials as low as $+1.6\ V_{RHE}$, although significant dissolution typically requires higher potentials.[305,306] The difference in the dissolution rates between IrO_2 and RuO_2 is also reflected in Figure 8, where Ru in the nanoparticulate form loses its activity and probably implies a complete dissolution of the Ru nanoparticles even after a single sweep.[224] Despite simply considering thermodynamics, the approach described above indicates that particular redox transitions can indeed provide hints for the interplay between activity and stability. Nevertheless, as the kinetics and the mechanism of noble metal oxide dissolution are in general not well understood, more experimental efforts will be necessary in the future.

4.2.3. Gas Phase—Induced Degradation

The formation of gas bubbles during the OER introduces different sources for performance loss:

1) The partial blockage of the electrode through bubble formation leads to a local increase in the actual current densities in areas which are still accessible, and these local current densities may be significantly higher than nominal ones.[250] These inhomogeneous conditions can have enormous effects on the stability of the electrode which would not occur under uniform operation.[307] Therefore, the type of porosity is important for the overall performance in the long run, as it influences the accessibility of regions of the nanostructured surface, as described in section 4.1.3.
2) In extreme cases, mechanical rupture of the catalyst coating may occur as a result of the high pressure of gas generated inside the pores of the catalytic material.[276]

4.3. Abundance of the Materials Used in OER Catalysts

Despite the low OER overpotential and decent stability of RuO_2 or IrO_2 under operation conditions, their use as electrocatalyst materials on a large scale is barely feasible due to their limited abundance in the Earth's crust and their related high cost.[184] The limited availability of these materials is a driver for the development of OER catalysts based on more-abundant, nonprecious elements. However, the stability of non-noble materials under the OER conditions is particularly critical in acidic media,[221] while their performance in neutral or alkaline solutions seems to be more promising. Moreover, materials based on less scarce (PbO_2) or abundant (Fe_3O_4) elements show large overpotentials for the OER.[220] The same is true for TiO_2, ZrO_2, SnO_2, Ta_2O_5, and CeO_2, which can nevertheless be used as the matrix for the catalytically active component. In contrast, MnO_2 and the less-abundant Co_3O_4 seem to have a significant potential to approach the activity of RuO_2 or IrO_2.[308]

Several efforts have been made to synthesize various forms of Co_3O_4 with different, preferential crystallographic planes to improve the activity and stability.[309] A very interesting attempt to design nanostructured Co-based catalysts for the OER, is the so-called in situ formed catalysts (Figure 11), which operate in neutral solutions under ambient

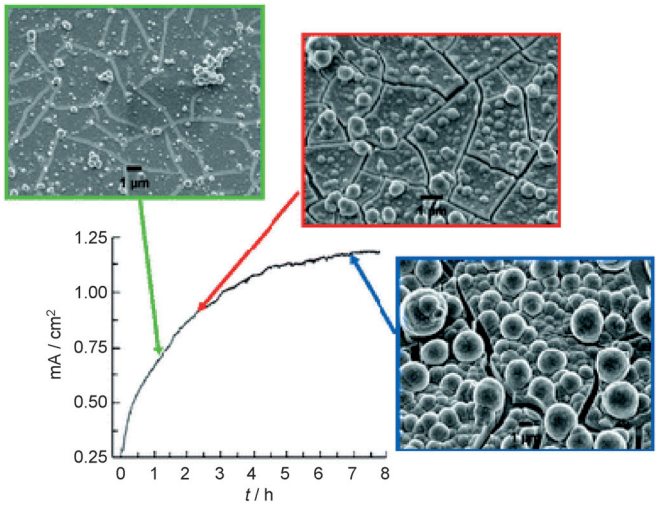

Figure 11. In situ formed Co-based catalyst: Current density profile for bulk electrolysis at +1.29 V (vs. NHE) in 0.1 M phosphate buffer (pH 7.0) containing 0.5 mM Co^{2+}. SEM images of the electrode surface taken at indicated time points during the electrodeposition of the catalyst film. Reprinted from Ref. [311] with permission from the Royal Society of Chemistry.

conditions.[310,311] The catalytic layer is deposited using a buffer solution containing Co^{2+} ions as a precursor,[312] while the nature of the electrolyte anions (e.g. borate, phosphate) is decisive for nanostructuring on a variety of substrates with complex geometries and high surface areas.[313–315] In principle, the activity of these catalysts is the same as that in acidic or alkaline media when the potential is expressed versus the pH-corrected RHE scale; however, the problem of the lower conductivity of neutral media has to be

addressed by using solutions of sufficiently high ionic strength. Nevertheless, the appealing "self-healing" phenomena of the in situ formed catalysts, where the electrolyte anions (e.g. phosphate) play a crucial role in recovering the Co-based (also extended to Ni-based) catalyst,[316,317] could mitigate the rupture of the catalyst surface, which is unavoidable when the oxide itself participates in the OER, thus assuring long-term operation.

On the other hand, MnO_x (formally MnO_2) is also promising considering the rich redox chemistry of Mn and its much better abundance in the Earth's crust compared to Co.[318] From experimental studies assisted by DFT calculations,[318] it has been suggested that nanostructured α-Mn_2O_3 is an excellent catalyst for the OER. The catalyst undergoes phase changes at the surface as a function of the applied potential. This suggests that a key aspect in understanding the behavior of Mn oxide catalysts is to understand the surface reconstruction at the electrochemical interface during the OER. Even though there is increasing interest in developing non-noble MnO_x-based electrodes,[319,320] much systematic work is still needed.

Last but not least, a tenfold increase in the OER activity compared to IrO_2 was achieved in alkaline media with a perovskite of the type $Ba_{0.5}Sr_{0.5}Co_{0.8}Fe_{0.2}O_{3-\delta}$.[222] The high activity of this catalyst was predicted by a design approach that combined a systematic investigation of the OER activity of various transition-metal oxides with molecular orbital modeling, and was confirmed by rotating ring-disc electrode and galvanostatic measurements. Structural changes from corner- to edge-sharing octahedra, which occurs during water oxidation for $Ba_{0.5}Sr_{0.5}Co_{0.8}Fe_{0.2}O_{3-\delta}$ and some other perovskites, have been associated with their impressive activity toward the OER.[321] The performance of such materials in the long term is expected to be of particular importance.[322,323]

5. Outlook and Future Challenges

The large-scale deployment of electrochemical energy conversion and storage technologies is currently limited by the severe challenges in the design of efficient catalysts for the OER and ORR, which directly affect the cost of the devices. The main deficiencies are related to:

1) the activity of the electrodes, as both oxygen reactions exhibit significant overpotential even on the most active catalysts known, thereby resulting in higher energy consumption for water splitting and in lower energy recovery for the recombination of H_2 and O_2;
2) the stability of the electrodes, as the OER and ORR catalysts are exposed to harsh conditions that are detrimental for the overall long-term performance of the electrochemical cell;
3) the abundance of the materials used, as the most active catalysts for the OER and the ORR are based on noble metals that are, in general, scarce and expensive.

Although specifically designed materials nowadays satisfy some of these requirements, developing nanostructured materials for the ORR and OER that address all three criteria under real conditions still remains an enormous challenge.

To advance the field it will thus be essential to identify and understand the complex fundamental interrelation between the material properties, the reactions of interest, the emerging degradation processes, the conditions of operation, and the real structure and composition of the electrode. Clearly, such a multidimensional problem can be addressed only with multidisciplinary approaches that will at least combine (Scheme 2):

1) materials science, for the controlled synthesis and characterization of the materials that dictate the catalyst performance;
2) fundamental electrochemistry, for the clear experimental and theoretical description of the related processes;
3) chemical engineering, for studying the complex effects of catalysis in structured electrodes and the performance of large-scale applications.

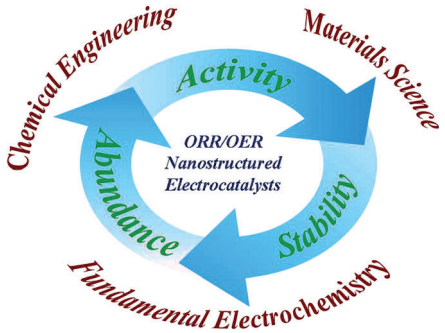

Scheme 2. A combined materials science, fundamental electrochemistry, and chemical engineering approach is required to address the issues of activity, stability, and abundance of the nanostructured OER and ORR electrocatalysts.

Of particular importance will be the further development and implementation of in situ methods for the investigation of, for example, the catalyst structure, composition, and electronic properties at all stages. Breakthrough developments in one of the above fields could of course make a tremendous contribution; however, only the concerted development will provide integrated solutions. Therefore, a promising strategy to develop and eventually implement sustainable technologies for the electrochemical conversion, storage, and utilization of energy relies on the systematic and joint study of the ORR and OER performance of catalysts with a reduced content of non-abundant noble materials.

We thank BMBF for supporting this work (Kz: 033RC1101 A) and A. Topalov for the preparation of the Frontispiece.

Received: July 28, 2013
Published online: December 11, 2013

[1] N. Armaroli, V. Balzani, *Angew. Chem.* **2007**, *119*, 52–67; *Angew. Chem. Int. Ed.* **2007**, *46*, 52–66.

[2] N. S. Lewis, D. G. Nocera, *Proc. Natl. Acad. Sci. USA* **2006**, *103*, 15729 – 15735.
[3] M. Z. Jacobson, *Energy Environ. Sci.* **2009**, *2*, 148 – 173.
[4] D. Gust, T. A. Moore, A. L. Moore, *Acc. Chem. Res.* **2009**, *42*, 1890 – 1898.
[5] Z. Yang, J. Zhang, M. C. W. Kintner-Meyer, X. Lu, D. Choi, J. P. Lemmon, J. Liu, *Chem. Rev.* **2011**, *111*, 3577 – 3613.
[6] P. G. Bruce, B. Scrosati, J.-M. Tarascon, *Angew. Chem.* **2008**, *120*, 2972 – 2989; *Angew. Chem. Int. Ed.* **2008**, *47*, 2930 – 2946.
[7] G. A. Olah, *Angew. Chem.* **2005**, *117*, 2692 – 2696; *Angew. Chem. Int. Ed.* **2005**, *44*, 2636 – 2639.
[8] Y. Hori in *Modern Aspects of Electrochemistry* (Ed.: C. Vayenas), Springer, New York, **2008**, pp. 89 – 189.
[9] S. Wasmus, A. Küver, *J. Electroanal. Chem.* **1999**, *461*, 14 – 31.
[10] J. O'M. Bockris, *Science* **1972**, *176*, 1323 – 1323.
[11] N. M. Markovic, P. N. Ross, *Surf. Sci. Rep.* **2002**, *45*, 117 – 229.
[12] F. Raimondi, G. G. Scherer, R. Kötz, A. Wokaun, *Angew. Chem.* **2005**, *117*, 2228 – 2248; *Angew. Chem. Int. Ed.* **2005**, *44*, 2190 – 2209.
[13] J. A. Cracknell, K. A. Vincent, F. A. Armstrong, *Chem. Rev.* **2008**, *108*, 2439 – 2461.
[14] S. C. Barton, J. Gallaway, P. Atanassov, *Chem. Rev.* **2004**, *104*, 4867 – 4886.
[15] V. Artero, M. Chavarot-Kerlidou, M. Fontecave, *Angew. Chem.* **2011**, *123*, 7376 – 7405; *Angew. Chem. Int. Ed.* **2011**, *50*, 7238 – 7266.
[16] G. N. Lewis, M. Randall, *J. Am. Chem. Soc.* **1914**, *36*, 1969 – 1993.
[17] I. Katsounaros, W. B. Schneider, J. C. Meier, U. Benedikt, P. U. Biedermann, A. A. Auer, K. J. J. Mayrhofer, *Phys. Chem. Chem. Phys.* **2012**, *14*, 7384 – 7391.
[18] I. Katsounaros, W. B. Schneider, J. C. Meier, U. Benedikt, P. U. Biedermann, A. Cuesta, A. A. Auer, K. J. J. Mayrhofer, *Phys. Chem. Chem. Phys.* **2013**, *15*, 8058 – 8068.
[19] M. Shao, P. Liu, R. R. Adzic, *J. Am. Chem. Soc.* **2006**, *128*, 7408 – 7409.
[20] T. Jacob, W. A. Goddard, *ChemPhysChem* **2006**, *7*, 992 – 1005.
[21] A. A. Topalov, I. Katsounaros, M. Auinger, S. Cherevko, J. C. Meier, S. O. Klemm, K. J. J. Mayrhofer, *Angew. Chem.* **2012**, *124*, 12782 – 12785; *Angew. Chem. Int. Ed.* **2012**, *51*, 12613 – 12615.
[22] S. Cherevko, A. A. Topalov, I. Katsounaros, K. J. J. Mayrhofer, *Electrochem. Commun.* **2013**, *28*, 44 – 46.
[23] J. Rossmeisl, A. Logadottir, J. K. Nørskov, *Chem. Phys.* **2005**, *319*, 178 – 184.
[24] I. C. Man, H.-Y. Su, F. Calle-Vallejo, H. A. Hansen, J. I. Martínez, N. G. Inoglu, J. Kitchin, T. F. Jaramillo, J. K. Nørskov, J. Rossmeisl, *ChemCatChem* **2011**, *3*, 1159 – 1165.
[25] F. Calle-Vallejo, J. I. Martínez, J. M. García-Lastra, J. Rossmeisl, M. T. M. Koper, *Phys. Rev. Lett.* **2012**, *108*, 116103.
[26] E. M. Fernández, P. G. Moses, A. Toftelund, H. A. Hansen, J. I. Martínez, F. Abild-Pedersen, J. Kleis, B. Hinnemann, J. Rossmeisl, T. Bligaard, J. K. Nørskov, *Angew. Chem.* **2008**, *120*, 4761 – 4764; *Angew. Chem. Int. Ed.* **2008**, *47*, 4683 – 4686.
[27] B. Hammer, J. K. Nørskov, *Nature* **1995**, *376*, 238 – 240.
[28] A. Nilsson, L. G. M. Pettersson, J. K. Nørskov, *Chemical Bonding at Surfaces and Interfaces*, Elsevier, Amsterdam, **2011**.
[29] B. Hammer, J. K. Nørskov, *Adv. Catal.* **2000**, *45*, 71 – 129.
[30] C. Lu, I. C. Lee, R. I. Masel, A. Wieckowski, C. Rice, *J. Phys. Chem. A* **2002**, *106*, 3084 – 3091.
[31] B. Huang, L. Zhuang, L. Xiao, J. Lu, *Chem. Sci.* **2013**, *4*, 606 – 611.
[32] E. Santos, P. Hindelang, P. Quaino, E. N. Schulz, G. Soldano, W. Schmickler, *ChemPhysChem* **2011**, *12*, 2274 – 2279.
[33] J. Rossmeisl, G. S. Karlberg, T. Jaramillo, J. K. Nørskov, *Faraday Discuss.* **2009**, *140*, 337 – 346.
[34] J. K. Nørskov, J. Rossmeisl, A. Logadottir, L. Lindqvist, J. R. Kitchin, T. Bligaard, H. Jonsson, *J. Phys. Chem. B* **2004**, *108*, 17886 – 17892.
[35] M. T. M. Koper, *J. Electroanal. Chem.* **2011**, *660*, 254 – 260.
[36] B. N. Grgur, N. M. Markovic, P. N. Ross, *Can. J. Chem.* **1997**, *75*, 1465 – 1471.
[37] D. Strmcnik, Active Sites for PEM Fuel Cell Reactions in Model and Real Systems, PhD Dissertation, Univerza v Ljubljani, **2007**.
[38] N. M. Markovic, H. A. Gasteiger, P. N. Ross, *J. Phys. Chem.* **1995**, *99*, 3411 – 3415.
[39] N. M. Markovic, H. A. Gasteiger, P. N. Ross, *J. Phys. Chem.* **1996**, *100*, 6715 – 6721.
[40] R. Van Hardeveld, F. Hartog, *Surf. Sci.* **1969**, *15*, 189 – 230.
[41] W. Romanowski, *Surf. Sci.* **1969**, *18*, 373 – 388.
[42] J. M. Montejano-Carrizales, F. Aguilera-Granja, J. L. Morán-López, *Nanostruct. Mater.* **1997**, *8*, 269 – 287.
[43] M. T. M. Koper, *Nanoscale* **2011**, *3*, 2054 – 2073.
[44] K. Kinoshita, *J. Electrochem. Soc.* **1990**, *137*, 845 – 848.
[45] S. Mukerjee, J. McBreen, *J. Electroanal. Chem.* **1998**, *448*, 163 – 171.
[46] G. A. Tritsaris, J. Greeley, J. Rossmeisl, J. K. Nørskov, *Catal. Lett.* **2011**, *141*, 909 – 913.
[47] M. Shao, A. Peles, K. Shoemaker, *Nano Lett.* **2011**, *11*, 3714 – 3719.
[48] F. J. Perez-Alonso, D. N. McCarthy, A. Nierhoff, P. Hernandez-Fernandez, C. Strebel, I. E. L. Stephens, J. H. Nielsen, I. Chorkendorff, *Angew. Chem.* **2012**, *124*, 4719 – 4721; *Angew. Chem. Int. Ed.* **2012**, *51*, 4641 – 4643.
[49] Y. Takasu, N. Ohashi, X.-G. Zhang, Y. Murakami, H. Minagawa, S. Sato, K. Yahikozawa, *Electrochim. Acta* **1996**, *41*, 2595 – 2600.
[50] H. A. Gasteiger, S. S. Kocha, B. Sompalli, F. T. Wagner, *Appl. Catal. B* **2005**, *56*, 9 – 35.
[51] K. J. J. Mayrhofer, B. B. Blizanac, M. Arenz, V. R. Stamenkovic, P. N. Ross, N. M. Markovic, *J. Phys. Chem. B* **2005**, *109*, 14433 – 14440.
[52] H. Yano, J. Inukai, H. Uchida, M. Watanabe, P. K. Babu, T. Kobayashi, J. H. Chung, E. Oldfield, A. Wieckowski, *Phys. Chem. Chem. Phys.* **2006**, *8*, 4932 – 4939.
[53] A. Sarapuu, A. Kasikov, T. Laaksonen, K. Kontturi, K. Tammeveski, *Electrochim. Acta* **2008**, *53*, 5873 – 5880.
[54] H. Ye, J. A. Crooks, R. M. Crooks, *Langmuir* **2007**, *23*, 11901 – 11906.
[55] K. J. J. Mayrhofer, D. Strmcnik, B. B. Blizanac, V. Stamenkovic, M. Arenz, N. M. Markovic, *Electrochim. Acta* **2008**, *53*, 3181 – 3188.
[56] M. Nesselberger, S. Ashton, J. C. Meier, I. Katsounaros, K. J. J. Mayrhofer, M. Arenz, *J. Am. Chem. Soc.* **2011**, *133*, 17428 – 17433.
[57] W. Sheng, S. Chen, E. Vescovo, Y. Shao-Horn, *J. Electrochem. Soc.* **2012**, *159*, B96 – B103.
[58] K. Ke, K. Hiroshima, Y. Kamitaka, T. Hatanaka, Y. Morimoto, *Electrochim. Acta* **2012**, *72*, 120 – 128.
[59] M. Nesselberger, M. Roefzaad, R. F. Hamou, P. U. Biedermann, F. F. Schweinberger, S. Kunz, K. Schloegl, G. K. H. Wiberg, S. Ashton, U. Heiz, K. J. J. Mayrhofer, M. Arenz, *Nat. Mater.* **2013**, *12*, 919 – 924.
[60] T. S. Ahmadi, Z. L. Wang, T. C. Green, A. Henglein, M. A. El-Sayed, *Science* **1996**, *272*, 1924 – 1925.
[61] A. Chen, P. Holt-Hindle, *Chem. Rev.* **2010**, *110*, 3767 – 3804.
[62] Z. Chen, M. Waje, W. Li, Y. Yan, *Angew. Chem.* **2007**, *119*, 4138 – 4141; *Angew. Chem. Int. Ed.* **2007**, *46*, 4060 – 4063.
[63] H. Zhou, W. Zhou, R. R. Adzic, S. S. Wong, *J. Phys. Chem. C* **2009**, *113*, 5460 – 5466.
[64] W. J. Khudhayer, A. U. Shaikh, T. Karabacak, *Adv. Sci. Lett.* **2011**, *4*, 3551 – 3559.

[65] J. Chen, B. Lim, E. P. Lee, Y. Xia, *Nano Today* **2009**, *4*, 81 – 95.
[66] M. Subhramannia, V. K. Pillai, *J. Mater. Chem.* **2008**, *18*, 5858 – 5870.
[67] V. Komanicky, H. Iddir, K.-C. Chang, A. Menzel, G. Karapetrov, D. Hennessy, P. Zapol, H. You, *J. Am. Chem. Soc.* **2009**, *131*, 5732 – 5733.
[68] C. M. Sánchez-Sánchez, J. Solla-Gullón, F. J. Vidal-Iglesias, A. Aldaz, V. Montiel, E. Herrero, *J. Am. Chem. Soc.* **2010**, *132*, 5622 – 5624.
[69] C. M. Sánchez-Sánchez, F. J. Vidal-Iglesias, J. Solla-Gullón, V. Montiel, A. Aldaz, J. M. Feliu, E. Herrero, *Electrochim. Acta* **2010**, *55*, 8252 – 8257.
[70] E. Antolini, J. Perez, *J. Mater. Sci.* **2011**, *46*, 4435 – 4457.
[71] V. Stamenkovic, B. S. Mun, K. J. J. Mayrhofer, P. N. Ross, N. M. Markovic, J. Rossmeisl, J. Greeley, J. K. Nørskov, *Angew. Chem.* **2006**, *118*, 2963 – 2967; *Angew. Chem. Int. Ed.* **2006**, *45*, 2897 – 2901.
[72] J. R. Kitchin, J. K. Nørskov, M. A. Barteau, J. G. Chen, *Phys. Rev. Lett.* **2004**, *93*, 156801.
[73] V. R. Stamenkovic, B. S. Mun, M. Arenz, K. J. J. Mayrhofer, C. A. Lucas, G. F. Wang, P. N. Ross, N. M. Markovic, *Nat. Mater.* **2007**, *6*, 241 – 247.
[74] S. R. Brankovic, J. X. Wang, R. R. Adžić, *Surf. Sci.* **2001**, *474*, L173 – L179.
[75] J. L. Zhang, M. B. Vukmirovic, Y. Xu, M. Mavrikakis, R. R. Adzic, *Angew. Chem.* **2005**, *117*, 2170 – 2173; *Angew. Chem. Int. Ed.* **2005**, *44*, 2132 – 2135.
[76] R. R. Adzic, J. Zhang, K. Sasaki, M. B. Vukmirovic, M. Shao, J. X. Wang, A. U. Nilekar, M. Mavrikakis, J. A. Valerio, F. Uribe, *Top. Catal.* **2007**, *46*, 249 – 262.
[77] M. B. Vukmirovic, J. Zhang, K. Sasaki, A. U. Nilekar, F. Uribe, M. Mavrikakis, R. R. Adzic, *Electrochim. Acta* **2007**, *52*, 2257 – 2263.
[78] V. R. Stamenkovic, B. S. Mun, K. J. J. Mayrhofer, P. N. Ross, N. M. Markovic, *J. Am. Chem. Soc.* **2006**, *128*, 8813 – 8819.
[79] V. R. Stamenkovic, B. Fowler, B. S. Mun, G. F. Wang, P. N. Ross, C. A. Lucas, N. M. Markovic, *Science* **2007**, *315*, 493 – 497.
[80] I. E. L. Stephens, A. S. Bondarenko, F. J. Perez-Alonso, F. Calle-Vallejo, L. Bech, T. P. Johansson, A. K. Jepsen, R. Frydendal, B. P. Knudsen, J. Rossmeisl, I. Chorkendorff, *J. Am. Chem. Soc.* **2011**, *133*, 5485 – 5491.
[81] A. S. Bondarenko, I. E. L. Stephens, L. Bech, I. Chorkendorff, *Electrochim. Acta* **2012**, *82*, 517 – 523.
[82] A. S. Bandarenka, A. S. Varela, M. Karamad, F. Calle-Vallejo, L. Bech, F. J. Perez-Alonso, J. Rossmeisl, I. E. L. Stephens, I. Chorkendorff, *Angew. Chem.* **2012**, *124*, 12015 – 12018; *Angew. Chem. Int. Ed.* **2012**, *51*, 11845 – 11848.
[83] R. Ferrando, J. Jellinek, R. L. Johnston, *Chem. Rev.* **2008**, *108*, 845 – 910.
[84] S. Guo, E. Wang, *Nano Today* **2011**, *6*, 240 – 264.
[85] M. Chen, J. P. Liu, S. Sun, *J. Am. Chem. Soc.* **2004**, *126*, 8394 – 8395.
[86] M. Min, J. Cho, K. Cho, H. Kim, *Electrochim. Acta* **2000**, *45*, 4211 – 4217.
[87] Y. Qian, W. Wen, P. A. Adcock, Z. Jiang, N. Hakim, M. S. Saha, S. Mukerjee, *J. Phys. Chem. C* **2008**, *112*, 1146 – 1157.
[88] M. K. Carpenter, T. E. Moylan, R. S. Kukreja, M. H. Atwan, M. M. Tessema, *J. Am. Chem. Soc.* **2012**, *134*, 8535 – 8542.
[89] S. Mukerjee, S. Srinivasan, M. P. Soriaga, J. McBreen, *J. Phys. Chem.* **1995**, *99*, 4577 – 4589.
[90] S. Mukerjee, S. Srinivasan, *J. Electroanal. Chem.* **1993**, *357*, 201 – 224.
[91] S. Mukerjee, S. Srinivasan, M. P. Soriaga, J. McBreen, *J. Electrochem. Soc.* **1995**, *142*, 1409 – 1422.
[92] U. A. Paulus, A. Wokaun, G. G. Scherer, T. J. Schmidt, V. Stamenkovic, N. M. Markovic, P. N. Ross, *Electrochim. Acta* **2002**, *47*, 3787 – 3798.
[93] U. A. Paulus, A. Wokaun, G. G. Scherer, T. J. Schmidt, V. Stamenkovic, V. Radmilovic, N. M. Markovic, P. N. Ross, *J. Phys. Chem. B* **2002**, *106*, 4181 – 4191.
[94] D. Wang, H. L. Xin, R. Hovden, H. Wang, Y. Yu, D. A. Muller, F. J. DiSalvo, H. D. Abruña, *Nat. Mater.* **2012**, *12*, 81 – 87.
[95] J. Wu, J. Zhang, Z. Peng, S. Yang, F. T. Wagner, H. Yang, *J. Am. Chem. Soc.* **2010**, *132*, 4984 – 4985.
[96] P. Mani, R. Srivastava, P. Strasser, *J. Phys. Chem. C* **2008**, *112*, 2770 – 2778.
[97] C. Wang, D. van der Vliet, K.-C. Chang, H. You, D. Strmcnik, J. A. Schlueter, N. M. Markovic, V. R. Stamenkovic, *J. Phys. Chem. C* **2009**, *113*, 19365 – 19368.
[98] C. Wang, M. Chi, G. Wang, D. van der Vliet, D. Li, K. More, H.-H. Wang, J. A. Schlueter, N. M. Markovic, V. R. Stamenkovic, *Adv. Funct. Mater.* **2011**, *21*, 147 – 152.
[99] C. Wang, N. M. Markovic, V. R. Stamenkovic, *ACS Catal.* **2012**, *2*, 891 – 898.
[100] S. Guo, S. Zhang, S. Sun, *Angew. Chem.* **2013**, *125*, 8686 – 8705; *Angew. Chem. Int. Ed.* **2013**, *52*, 8526 – 8544.
[101] B. C. Beard, P. N. Ross, *J. Electrochem. Soc.* **1990**, *137*, 3368 – 3374.
[102] P. Strasser, S. Koh, T. Anniyev, J. Greeley, K. More, C. Yu, Z. Liu, S. Kaya, D. Nordlund, H. Ogasawara, M. F. Toney, A. Nilsson, *Nat. Chem.* **2010**, *2*, 454 – 460.
[103] P. Strasser, *Rev. Chem. Eng.* **2009**, *25*, 255 – 295.
[104] R. Srivastava, P. Mani, N. Hahn, P. Strasser, *Angew. Chem.* **2007**, *119*, 9146 – 9149; *Angew. Chem. Int. Ed.* **2007**, *46*, 8988 – 8991.
[105] S. Koh, P. Strasser, *J. Am. Chem. Soc.* **2007**, *129*, 12624 – 12625.
[106] K. C. Neyerlin, R. Srivastava, C. Yu, P. Strasser, *J. Power Sources* **2009**, *186*, 261 – 267.
[107] D. Wang, Y. Yu, H. L. Xin, R. Hovden, P. Ercius, J. A. Mundy, H. Chen, J. H. Richard, D. A. Muller, F. J. DiSalvo, H. D. Abruña, *Nano Lett.* **2012**, *12*, 5230 – 5238.
[108] R. Yang, J. Leisch, P. Strasser, M. F. Toney, *Chem. Mater.* **2010**, *22*, 4712 – 4720.
[109] M. Oezaslan, M. Heggen, P. Strasser, *J. Am. Chem. Soc.* **2012**, *134*, 514 – 524.
[110] Z. Yu, J. Zhang, Z. Liu, J. M. Ziegelbauer, H. Xin, I. Dutta, D. A. Muller, F. T. Wagner, *J. Phys. Chem. C* **2012**, *116*, 19877 – 19885.
[111] F. T. Wagner, B. Lakshmanan, M. F. Mathias, *J. Phys. Chem. Lett.* **2010**, *1*, 2204 – 2219.
[112] F. A. de Bruijn, V. A. T. Dam, G. J. M. Janssen, *Fuel Cells* **2008**, *8*, 3 – 22.
[113] The U. S. Department of Energy, "Fuel cell technologies office multi-year research, development and demonstration plan—Technical Plan: Fuel Cells," can be found under http://www1.eere.energy.gov/hydrogenandfuelcells/mypp/pdfs/fuel_cells.pdf, **2011**.
[114] R. Borup, J. Meyers, B. Pivovar, Y. S. Kim, R. Mukundan, N. Garland, D. Myers, M. Wilson, F. Garzon, D. Wood, P. Zelenay, K. More, K. Stroh, T. Zawodzinski, J. Boncella, J. E. McGrath, M. Inaba, K. Miyatake, M. Hori, K. Ota, Z. Ogumi, S. Miyata, A. Nishikata, Z. Siroma, Y. Uchimoto, K. Yasuda, K. Kimijima, N. Iwashita, *Chem. Rev.* **2007**, *107*, 3904 – 3951.
[115] J. C. Meier, C. Galeano, I. Katsounaros, A. A. Topalov, A. Kostka, F. Schüth, K. J. J. Mayrhofer, *ACS Catal.* **2012**, *2*, 832 – 843.
[116] J. C. Meier, I. Katsounaros, C. Galeano, H. J. Bongard, A. A. Topalov, A. Kostka, A. Karschin, F. Schüth, K. J. J. Mayrhofer, *Energy Environ. Sci.* **2012**, *5*, 9319 – 9330.
[117] Y. Shao-Horn, W. C. Sheng, S. Chen, P. J. Ferreira, E. F. Holby, D. Morgan, *Top. Catal.* **2007**, *46*, 285 – 305.
[118] L. Tang, B. Han, K. Persson, C. Friesen, T. He, K. Sieradzki, G. Ceder, *J. Am. Chem. Soc.* **2010**, *132*, 596 – 600.

[119] F. J. Perez-Alonso, C. F. Elkjaer, S. S. Shim, B. L. Abrams, I. E. L. Stephens, I. Chorkendorff, *J. Power Sources* **2011**, *196*, 6085 – 6091.
[120] S. Mukerjee, S. Srinivasan, *Handbook of Fuel Cells*: *Fundamentals*, *Technology*, *Applications* (Eds.: W. Vielstich, A. Lamm, H. A. Gasteiger), Wiley, Chichchester, **2003**, p. 503.
[121] J. A. S. Bett, K. Kinoshita, P. Stonehart, *J. Catal.* **1976**, *41*, 124 – 133.
[122] P. N. Ross in *Catalyst Deactivation* (Eds.: E. E. Petersen, A. T. Bell), Marcel Dekker, New York, **1987**, p. 165.
[123] J. Aragane, H. Urushibata, T. Murahashi, *J. Appl. Electrochem.* **1996**, *26*, 147 – 152.
[124] P. J. Ferreira, G. J. la O', Y. Shao-Horn, D. Morgan, R. Makharia, S. Kocha, H. A. Gasteiger, *J. Electrochem. Soc.* **2005**, *152*, A2256 – A2271.
[125] K. Kinoshita, J. T. Lundquist, P. Stonehart, *J. Electroanal. Chem.* **1973**, *48*, 157 – 166.
[126] K.-I. Ota, S. Nishigori, N. Kamiya, *J. Electroanal. Chem.* **1988**, *257*, 205 – 215.
[127] X. Wang, R. Kumar, D. J. Myers, *Electrochem. Solid-State Lett.* **2006**, *9*, A225 – A227.
[128] D. C. Johnson, D. T. Napp, S. Bruckenstein, *Electrochim. Acta* **1970**, *15*, 1493 – 1509.
[129] A. P. Yadav, A. Nishikata, T. Tsuru, *J. Electrochem. Soc.* **2009**, *156*, C253 – C258.
[130] M. Umeda, Y. Kuwahara, A. Nakazawa, M. Inoue, *J. Phys. Chem. C* **2009**, *113*, 15707 – 15713.
[131] D. A. J. Rand, R. Woods, *J. Electroanal. Chem.* **1972**, *35*, 209 – 218.
[132] G. Inzelt, B. Berkes, Á. Kriston, *Electrochim. Acta* **2010**, *55*, 4742 – 4749.
[133] R. M. Darling, J. P. Meyers, *J. Electrochem. Soc.* **2003**, *150*, A1523 – A1527.
[134] R. M. Darling, J. P. Meyers, *J. Electrochem. Soc.* **2005**, *152*, A242 – A247.
[135] G. Jerkiewicz, G. Vatankhah, J. Lessard, M. P. Soriaga, Y.-S. Park, *Electrochim. Acta* **2004**, *49*, 1451 – 1459.
[136] Z. Nagy, H. You, *Electrochim. Acta* **2002**, *47*, 3037 – 3055.
[137] M. Wakisaka, S. Asizawa, H. Uchida, M. Watanabe, *Phys. Chem. Chem. Phys.* **2010**, *12*, 4184 – 4190.
[138] S. O. Klemm, A. Karschin, A. K. Schuppert, A. A. Topalov, A. M. Mingers, I. Katsounaros, K. J. J. Mayrhofer, *J. Electroanal. Chem.* **2012**, *677*, 50 – 55.
[139] J. Zhang, K. Sasaki, E. Sutter, R. R. Adzic, *Science* **2007**, *315*, 220 – 222.
[140] S. G. Rinaldo, J. Stumper, M. Eikerling, *J. Phys. Chem. C* **2010**, *114*, 5773 – 5785.
[141] E. F. Holby, D. Morgan, *J. Electrochem. Soc.* **2012**, *159*, B578 – B591.
[142] E. F. Holby, W. Sheng, Y. Shao-Horn, D. Morgan, *Energy Environ. Sci.* **2009**, *2*, 865 – 871.
[143] N. Hodnik, M. Zorko, B. Jozinović, M. Bele, G. Dražič, S. Hočevar, M. Gaberšček, *Electrochem. Commun.* **2013**, *30*, 75 – 78.
[144] M. Pourbaix, *Atlas of Electrochemical Equilibria in Aqueous Solutions*, Pergamon, Brussels, **1966**.
[145] K. Kinoshita, *Carbon—Electrochemical and Physicochemical Properties*, Wiley, New York, **1988**.
[146] F. A. Heckman, D. F. Harling, *Rubber Chem. Technol.* **1966**, *39*, 1 – 13.
[147] K. Kinoshita, J. Bett, *Carbon* **1973**, *11*, 237 – 247.
[148] G. A. Gruver, *J. Electrochem. Soc.* **1978**, *125*, 1719 – 1720.
[149] K. Schlögl, K. J. J. Mayrhofer, M. Hanzlik, M. Arenz, *J. Electroanal. Chem.* **2011**, *662*, 355 – 360.
[150] Z. Y. Liu, J. L. Zhang, P. T. Yu, J. X. Zhang, R. Makharia, K. L. More, E. A. Stach, *J. Electrochem. Soc.* **2010**, *157*, B906 – B913.
[151] H. Schulenburg, B. Schwanitz, N. Linse, G. G. Scherer, A. Wokaun, J. Krbanjevic, R. Grothausmann, I. Manke, *J. Phys. Chem. C* **2011**, *115*, 14236 – 14243.
[152] S. Shrestha, Y. Liu, W. E. Mustain, *Catal. Rev. Sci. Eng.* **2011**, *53*, 256 – 336.
[153] J. Kim, S. W. Lee, C. Carlton, Y. Shao-Horn, *J. Phys. Chem. Lett.* **2011**, *2*, 1332 – 1336.
[154] F. Hasché, M. Oezaslan, P. Strasser, *Phys. Chem. Chem. Phys.* **2010**, *12*, 15251 – 15258.
[155] B. Seger, P. V. Kamat, *J. Phys. Chem. C* **2009**, *113*, 7990 – 7995.
[156] D. Banham, F. Feng, K. Pei, S. Ye, V. Birss, *J. Mater. Chem. A* **2013**, *1*, 2812 – 2820.
[157] S. H. Joo, S. J. Choi, I. Oh, J. Kwak, Z. Liu, O. Terasaki, R. Ryoo, *Nature* **2001**, *412*, 169 – 172.
[158] C. Galeano, J. C. Meier, V. Peinecke, H. Bongard, I. Katsounaros, A. A. Topalov, A. Lu, K. J. J. Mayrhofer, F. Schüth, *J. Am. Chem. Soc.* **2012**, *134*, 20457 – 20465.
[159] F. Alcaide, G. Álvarez, O. Miguel, M. J. Lázaro, R. Moliner, A. López-Cudero, J. Solla-Gullón, E. Herrero, A. Aldaz, *Electrochem. Commun.* **2009**, *11*, 1081 – 1084.
[160] J. Marie, S. Berthon-Fabry, P. Achard, M. Chatenet, A. Pradourat, E. Chainet, *J. Non-Cryst. Solids* **2004**, *350*, 88 – 96.
[161] S. Andersson, B. Collén, U. Kuylenstierna, A. Magnéli, *Acta Chem. Scand.* **1957**, *11*, 1641 – 1652.
[162] J. M. Jaksic, D. Labou, G. D. Papakonstantinou, A. Siokou, M. M. Jaksic, *J. Phys. Chem. C* **2010**, *114*, 18298 – 18312.
[163] S. G. Neophytides, K. Murase, S. Zafeiratos, G. Papakonstantinou, F. E. Paloukis, N. V. Krstajic, M. M. Jaksic, *J. Phys. Chem. B* **2006**, *110*, 3030 – 3042.
[164] M. K. Debe, A. K. Schmoeckel, G. D. Vernstrom, R. Atanasoski, *J. Power Sources* **2006**, *161*, 1002 – 1011.
[165] M. K. Debe, R. T. Atanasoski, A. J. Steinbach, *ECS Trans.* **2011**, 937 – 954.
[166] Y. Yu, H. L. Xin, R. Hovden, D. Wang, E. D. Rus, J. A. Mundy, D. A. Muller, H. D. Abruña, *Nano Lett.* **2012**, *12*, 4417 – 4423.
[167] J. C. Meier, C. Galeano, I. Katsounaros, J. Witte, H. J. Bongard, A. A. Topalov, C. Baldizzone, S. Mezzavilla, F. Schüth, K. J. J. Mayrhofer, *Beilstein J. Nanotechnol.* **2013**, submitted.
[168] K. Hartl, M. Hanzlik, M. Arenz, *Energy Environ. Sci.* **2011**, *4*, 234 – 238.
[169] E. Ruckenstein, B. Pulvermacher, *J. Catal.* **1973**, *29*, 224 – 245.
[170] K. J. J. Mayrhofer, J. C. Meier, S. J. Ashton, G. K. H. Wiberg, F. Kraus, M. Hanzlik, M. Arenz, *Electrochem. Commun.* **2008**, *10*, 1144 – 1147.
[171] K. J. J. Mayrhofer, S. J. Ashton, J. C. Meier, G. K. H. Wiberg, M. Hanzlik, M. Arenz, *J. Power Sources* **2008**, *185*, 734 – 739.
[172] K. Schlögl, M. Hanzlik, M. Arenz, *J. Electrochem. Soc.* **2012**, *159*, B677 – B682.
[173] W. B. Schneider, U. Benedikt, A. A. Auer, *ChemPhysChem* **2013**, *14*, 2984 – 2989.
[174] K. Jayasayee, J. A. R. V. Veen, T. G. Manivasagam, S. Celebi, E. J. M. Hensen, F. A. de Bruijn, *Appl. Catal. B* **2012**, *111*, 515 – 526.
[175] C. E. Carlton, S. Chen, P. J. Ferreira, L. F. Allard, Y. Shao-Horn, *J. Phys. Chem. Lett.* **2012**, *3*, 161 – 166.
[176] T. Okada, Y. Ayato, M. Yuasa, I. Sekine, *J. Phys. Chem. B* **1999**, *103*, 3315 – 3322.
[177] J. Erlebacher, M. J. Aziz, A. Karma, N. Dimitrov, K. Sieradzki, *Nature* **2001**, *410*, 450 – 453.
[178] P. B. Balbuena, R. Callejas-Tovar, P. Hirunsit, J. M. Martínez de La Hoz, Y. Ma, G. E. Ramírez-Caballero, *Top. Catal.* **2012**, *55*, 322 – 335.
[179] K. J. J. Mayrhofer, K. Hartl, V. Juhart, M. Arenz, *J. Am. Chem. Soc.* **2009**, *131*, 16348 – 16349.
[180] J. Greeley, I. E. L. Stephens, A. S. Bondarenko, T. P. Johansson, H. A. Hansen, T. F. Jaramillo, J. Rossmeisl, I. Chorkendorff, J. K. Nørskov, *Nat. Chem.* **2009**, *1*, 552 – 556.

[181] I. E. L. Stephens, A. S. Bondarenko, L. Bech, I. Chorkendorff, *ChemCatChem* **2012**, *4*, 341 – 349.
[182] M. Escudero-Escribano, A. Verdaguer-Casadevall, P. Malacrida, U. Grønbjerg, B. P. Knudsen, A. K. Jepsen, J. Rossmeisl, I. E. L. Stephens, I. Chorkendorff, *J. Am. Chem. Soc.* **2012**, *134*, 16476 – 16479.
[183] A. Marcu, G. Toth, R. Srivastava, P. Strasser, *J. Power Sources* **2012**, *208*, 288 – 295.
[184] P. C. K. Vesborg, T. F. Jaramillo, *RSC Adv.* **2012**, *2*, 7933 – 7947.
[185] A. Morozan, B. Jousselme, S. Palacin, *Energy Environ. Sci.* **2011**, *4*, 1238 – 1254.
[186] N. Ramaswamy, S. Mukerjee, *J. Phys. Chem. C* **2011**, *115*, 18015 – 18026.
[187] R. Jasinski, *Nature* **1964**, *201*, 1212 – 1213.
[188] R. Jasinski, *J. Electrochem. Soc.* **1965**, *112*, 526 – 528.
[189] H. Alt, H. Binder, G. Sandstede, *J. Catal.* **1973**, *28*, 8 – 19.
[190] A. Bettelheim, R. J. H. Chan, T. Kuwana, *J. Electroanal. Chem.* **1979**, *99*, 391 – 397.
[191] J. Zagal, M. Páez, A. A. Tanaka, J. R. dos Santos, Jr., C. A. Linkous, *J. Electroanal. Chem.* **1992**, *339*, 13 – 30.
[192] S. Gupta, D. Tryk, I. Bae, W. Aldred, E. Yeager, *J. Appl. Electrochem.* **1989**, *19*, 19 – 27.
[193] K. Wiesener, *Electrochim. Acta* **1986**, *31*, 1073 – 1078.
[194] K. Gong, F. Du, Z. Xia, M. Durstock, L. Dai, *Science* **2009**, *323*, 760 – 764.
[195] V. Nallathambi, J.-W. Lee, S. P. Kumaraguru, G. Wu, B. N. Popov, *J. Power Sources* **2008**, *183*, 34 – 42.
[196] P. H. Matter, U. S. Ozkan, *Catal. Lett.* **2006**, *109*, 115 – 123.
[197] M. S. Thorum, J. M. Hankett, A. A. Gewirth, *J. Phys. Chem. Lett.* **2011**, *2*, 295 – 298.
[198] H. Wang, R. Côté, G. Faubert, D. Guay, J. P. Dodelet, *J. Phys. Chem. B* **1999**, *103*, 2042 – 2049.
[199] R. Bashyam, P. Zelenay, *Nature* **2006**, *443*, 63 – 66.
[200] M. Lefèvre, E. Proietti, F. Jaouen, J.-P. Dodelet, *Science* **2009**, *324*, 71 – 74.
[201] G. Wu, K. L. More, C. M. Johnston, P. Zelenay, *Science* **2011**, *332*, 443 – 447.
[202] Y. Tang, B. L. Allen, D. R. Kauffman, A. Star, *J. Am. Chem. Soc.* **2009**, *131*, 13200 – 13201.
[203] R. Liu, D. Wu, X. Feng, K. Müllen, *Angew. Chem.* **2010**, *122*, 2619 – 2623; *Angew. Chem. Int. Ed.* **2010**, *49*, 2565 – 2569.
[204] E. Proietti, F. Jaouen, M. Lefèvre, N. Larouche, J. Tian, J. Herranz, J.-P. Dodelet, *Nat. Commun.* **2011**, *2*, 416.
[205] H. R. Byon, J. Suntivich, Y. Shao-Horn, *Chem. Mater.* **2011**, *23*, 3421 – 3428.
[206] A. Serov, M. H. Robson, B. Halevi, K. Artyushkova, P. Atanassov, *Electrochem. Commun.* **2012**, *22*, 53 – 56.
[207] S. Ma, G. A. Goenaga, A. V. Call, D.-J. Liu, *Chem. Eur. J.* **2011**, *17*, 2063 – 2067.
[208] T. S. Olson, S. Pylypenko, P. Atanassov, K. Asazawa, K. Yamada, H. Tanaka, *J. Phys. Chem. C* **2010**, *114*, 5049 – 5059.
[209] T. S. Olson, S. Pylypenko, J. E. Fulghum, P. Atanassov, *J. Electrochem. Soc.* **2010**, *157*, B54 – B63.
[210] J. Herranz, F. Jaouen, M. Lefèvre, U. I. Kramm, E. Proietti, J.-P. Dodelet, P. Bogdanoff, S. Fiechter, I. Abs-Wurmbach, P. Bertrand, T. M. Arruda, S. Mukerjee, *J. Phys. Chem. C* **2011**, *115*, 16087 – 16097.
[211] Z. Shi, H. Liu, K. Lee, E. Dy, J. Chlistunoff, M. Blair, P. Zelenay, J. Zhang, Z.-S. Liu, *J. Phys. Chem. C* **2011**, *115*, 16672 – 16680.
[212] U. I. Kramm, J. Herranz, N. Larouche, T. M. Arruda, M. Lefèvre, F. Jaouen, P. Bogdanoff, S. Fiechter, I. Abs-Wurmbach, S. Mukerjee, J.-P. Dodelet, *Phys. Chem. Chem. Phys.* **2012**, *14*, 11673 – 11688.
[213] F. Jaouen, E. Proietti, M. Lefèvre, R. Chenitz, J.-P. Dodelet, G. Wu, H. T. Chung, C. M. Johnston, P. Zelenay, *Energy Environ. Sci.* **2011**, *4*, 114 – 130.
[214] Z. Chen, D. Higgins, A. Yu, L. Zhang, J. Zhang, *Energy Environ. Sci.* **2011**, *4*, 3167 – 3192.
[215] M. Wohlfahrt-Mehrens, J. Heitbaum, *J. Electroanal. Chem.* **1987**, *237*, 251 – 260.
[216] S. Fierro, T. Nagel, H. Baltruschat, C. Comninellis, *Electrochem. Commun.* **2007**, *9*, 1969 – 1974.
[217] O. Diaz-Morales, F. Calle-Vallejo, C. de Munck, M. T. M. Koper, *Chem. Sci.* **2013**, *4*, 2334 – 2343.
[218] J. Rossmeisl, Z.-W. Qu, H. Zhu, G.-J. Kroes, J. K. Nørskov, *J. Electroanal. Chem.* **2007**, *607*, 83 – 89.
[219] H. Dau, C. Limberg, T. Reier, M. Risch, S. Roggan, P. Strasser, *ChemCatChem* **2010**, *2*, 724 – 761.
[220] S. Trasatti, *Electrochim. Acta* **1984**, *29*, 1503 – 1512.
[221] J. O'M. Bockris, T. Otagawa, *J. Electrochem. Soc.* **1984**, *131*, 290 – 302.
[222] J. Suntivich, K. J. May, H. A. Gasteiger, J. B. Goodenough, Y. Shao-Horn, *Science* **2011**, *334*, 1383 – 1385.
[223] Y. Matsumoto, E. Sato, *Mater. Chem. Phys.* **1986**, *14*, 397 – 426.
[224] T. Reier, M. Oezaslan, P. Strasser, *ACS Catal.* **2012**, *2*, 1765 – 1772.
[225] K. Zeng, D. Zhang, *Prog. Energy Combust. Sci.* **2010**, *36*, 307 – 326.
[226] A. Ursua, L. M. Gandia, P. Sanchis, *Proc. IEEE* **2012**, *100*, 410 – 426.
[227] P. Castelli, S. Trasatti, F. H. Pollak, W. E. O'Grady, *J. Electroanal. Chem.* **1986**, *210*, 189 – 194.
[228] Y. Lee, J. Suntivich, K. J. May, E. E. Perry, Y. Shao-Horn, *J. Phys. Chem. Lett.* **2012**, *3*, 399 – 404.
[229] E. Guerrini, S. Trasatti, *Russ. J. Electrochem.* **2006**, *42*, 1017 – 1025.
[230] J. Jirkovský, M. Makarova, P. Krtil, *Electrochem. Commun.* **2006**, *8*, 1417 – 1422.
[231] K. Macounová, J. Jirkovský, M. V. Makarova, J. Franc, P. Krtil, *J. Solid State Electrochem.* **2009**, *13*, 959 – 965.
[232] J. C. Cruz, V. Baglio, S. Siracusano, V. Antonucci, A. S. Aricò, R. Ornelas, L. Ortiz-Frade, G. Osorio-Monreal, S. M. Durón-Torres, L. G. Arriaga, *Int. J. Electrochem. Sci.* **2011**, *6*, 6607 – 6619.
[233] J. Jirkovský, H. Hoffmannová, M. Klementová, P. Krtil, *J. Electrochem. Soc.* **2006**, *153*, E111 – E118.
[234] E. Rasten, G. Hagen, R. Tunold, *Electrochim. Acta* **2003**, *48*, 3945 – 3952.
[235] R. E. Fuentes, S. Rau, T. Smolinka, J. W. Weidner, *ECS Trans.* **2010**, *28*, 23 – 35.
[236] R. E. Fuentes, J. Farell, J. W. Weidner, *Electrochem. Solid-State Lett.* **2011**, *14*, E5 – E7.
[237] R. Chen, V. Trieu, A. R. Zeradjanin, H. Natter, D. Teschner, J. Kintrup, A. Bulan, W. Schuhmann, R. Hempelmann, *Phys. Chem. Chem. Phys.* **2012**, *14*, 7392 – 7399.
[238] A. R. Zeradjanin, T. Schilling, S. Seisel, M. Bron, W. Schuhmann, *Anal. Chem.* **2011**, *83*, 7645 – 7650.
[239] H. Over, *Electrochim. Acta* **2013**, *93*, 314 – 333.
[240] A. Minguzzi, M. A. Alpuche-Aviles, J. R. López, S. Rondinini, A. J. Bard, *Anal. Chem.* **2008**, *80*, 4055 – 4064.
[241] L.-Å. Näslund, C. M. Sánchez-Sánchez, Á. S. Ingason, J. Bäckström, E. Herrero, J. Rosen, S. Holmin, *J. Phys. Chem. C* **2013**, *117*, 6126 – 6135.
[242] H. Wendt, *Electrochim. Acta* **1994**, *39*, 1749 – 1756.
[243] S. Ardizzone, G. Fregonara, S. Trasatti, *Electrochim. Acta* **1990**, *35*, 263 – 267.
[244] K. P. de Jong, J. Zečević, H. Friedrich, P. E. de Jongh, M. Bulut, S. van Donk, R. Kenmogne, A. Finiels, V. Hulea, F. Fajula, *Angew. Chem.* **2010**, *122*, 10272 – 10276; *Angew. Chem. Int. Ed.* **2010**, *49*, 10074 – 10078.
[245] D. R. Rolison, *Science* **2003**, *299*, 1698 – 1701.
[246] J. Koresh, A. Soffer, *J. Electrochem. Soc.* **1977**, *124*, 1379 – 1385.
[247] H. Vogt, *Electrochim. Acta* **1984**, *29*, 167 – 173.

[248] H. Vogt, *J. Appl. Electrochem.* **1993**, *23*, 1323 – 1325.
[249] N. P. Brandon, G. H. Kelsall, *J. Appl. Electrochem.* **1985**, *15*, 475 – 484.
[250] H. Vogt, *Electrochim. Acta* **2012**, *78*, 183 – 187.
[251] A. R. Zeradjanin, F. La Mantia, J. Masa, W. Schuhmann, *Electrochim. Acta* **2012**, *82*, 408 – 414.
[252] A. R. Zeradjanin, E. Ventosa, A. S. Bondarenko, W. Schuhmann, *ChemSusChem* **2012**, *5*, 1905 – 1911.
[253] R. Chen, V. Trieu, B. Schley, H. Natter, J. Kintrup, A. Bulan, R. Weber, R. Hempelmann, *Z. Phys. Chem.* **2013**, *227*, 651 – 666.
[254] V. Trieu, B. Schley, H. Natter, J. Kintrup, A. Bulan, R. Hempelmann, *Electrochim. Acta* **2012**, *78*, 188 – 194.
[255] R. S. Yeo, J. Orehotsky, W. Visscher, S. Srinivasan, *J. Electrochem. Soc.* **1981**, *128*, 1900 – 1904.
[256] R. Kötz, S. Stucki, *Electrochim. Acta* **1986**, *31*, 1311 – 1316.
[257] J. Pérez-Ramírez, C. Mondelli, T. Schmidt, O. F.-K. Schlüter, A. Wolf, L. Mleczko, T. Dreier, *Energy Environ. Sci.* **2011**, *4*, 4786 – 4799.
[258] J. A. Rodriguez, D. W. Goodman, *Science* **1992**, *257*, 897 – 903.
[259] Y. E. Roginskaya, O. V. Morozova, E. N. Loubnin, A. V. Popov, Y. I. Ulitina, V. V. Zhurov, S. A. Ivanov, S. Trasatti, *J. Chem. Soc. Faraday Trans.* **1993**, *89*, 1707 – 1715.
[260] E. N. Balko, P. H. Nguyen, *J. Appl. Electrochem.* **1991**, *21*, 678 – 682.
[261] K. Kadakia, M. K. Datta, O. I. Velikokhatnyi, P. Jampani, S. K. Park, P. Saha, J. A. Poston, A. Manivannan, P. N. Kumta, *Int. J. Hydrogen Energy* **2012**, *37*, 3001 – 3013.
[262] M. K. Datta, K. Kadakia, O. I. Velikokhatnyi, P. H. Jampani, S. J. Chung, J. A. Poston, A. Manivannan, P. N. Kumta, *J. Mater. Chem. A* **2013**, *1*, 4026 – 4037.
[263] N. Mamaca, E. Mayousse, S. Arrii-Clacens, T. W. Napporn, K. Servat, N. Guillet, K. B. Kokoh, *Appl. Catal. B* **2012**, *111 – 112*, 376 – 380.
[264] C. Angelinetta, S. Trasatti, L. D. Atanasoska, Z. S. Minevski, R. T. Atanasoski, *Mater. Chem. Phys.* **1989**, *22*, 231 – 247.
[265] M. Rubel, R. Haasch, P. Mrozek, A. Wieckowski, C. De Pauli, S. Trasatti, *Vacuum* **1994**, *45*, 423 – 427.
[266] F. I. Mattos-Costa, P. de Lima-Neto, S. A. S. Machado, L. A. Avaca, *Electrochim. Acta* **1998**, *44*, 1515 – 1523.
[267] S. Ardizzone, M. Falciola, S. Trasatti, *J. Electrochem. Soc.* **1989**, *136*, 1545 – 1550.
[268] R. D. Shannon, *Solid State Commun.* **1968**, *6*, 139 – 143.
[269] Y. E. Roginskaya, I. D. Belova, B. S. Galyamov, F. K. Chibirova, R. R. Shiprina, *Mater. Chem. Phys.* **1989**, *22*, 203 – 229.
[270] S. Gottesfeld, S. Srinivasan, *J. Electroanal. Chem.* **1978**, *86*, 89 – 104.
[271] J.-M. Hu, J.-Q. Zhang, C.-N. Cao, *Int. J. Hydrogen Energy* **2004**, *29*, 791 – 797.
[272] D. K. Bediako, Y. Surendranath, D. G. Nocera, *J. Am. Chem. Soc.* **2013**, *135*, 3662 – 3674.
[273] Q. Liu, J. Jin, J. Zhang, *ACS Appl. Mater. Interfaces* **2013**, *5*, 5002 – 5008.
[274] R. Subbaraman, D. Tripkovic, K.-C. Chang, D. Strmcnik, A. P. Paulikas, P. Hirunsit, M. Chan, J. Greeley, V. Stamenkovic, N. M. Markovic, *Nat. Mater.* **2012**, *11*, 550 – 557.
[275] R. L. Doyle, M. E. G. Lyons, *Phys. Chem. Chem. Phys.* **2013**, *15*, 5224 – 5237.
[276] G. N. Martelli, R. Ornelas, G. Faita, *Electrochim. Acta* **1994**, *39*, 1551 – 1558.
[277] S. Fierro, A. Kapałka, C. Comninellis, *Electrochem. Commun.* **2010**, *12*, 172 – 174.
[278] L. Ouattara, S. Fierro, O. Frey, M. Koudelka, C. Comninellis, *J. Appl. Electrochem.* **2009**, *39*, 1361 – 1367.
[279] R. T. Atanasoski, L. L. Atanasoska, D. A. Cullen, G. M. Haugen, K. L. More, G. D. Vernstrom, *Electrocatalysis* **2012**, *3*, 284 – 297.
[280] R. T. Atanasoski, L. L. Atanasoska, D. A. Cullen, *Electrocatalysis in Fuel Cells* (Ed.: M. Shao), Springer, London, **2013**, pp. 637 – 663.
[281] J. C. Cruz, V. Baglio, S. Siracusano, R. Ornelas, L. Ortiz-Frade, L. G. Arriaga, V. Antonucci, A. S. Aricò, *J. Nanopart. Res.* **2011**, *13*, 1639 – 1646.
[282] S. Song, H. Zhang, X. Ma, Z. Shao, R. T. Baker, B. Yi, *Int. J. Hydrogen Energy* **2008**, *33*, 4955 – 4961.
[283] J. K. Nørskov, T. Bligaard, J. Rossmeisl, C. H. Christensen, *Nat. Chem.* **2009**, *1*, 37 – 46.
[284] K. C. Neyerlin, G. Bugosh, R. Forgie, Z. Liu, P. Strasser, *J. Electrochem. Soc.* **2009**, *156*, B363 – B369.
[285] R. Forgie, G. Bugosh, K. C. Neyerlin, Z. Liu, P. Strasser, *Electrochem. Solid-State Lett.* **2010**, *13*, B36 – B39.
[286] G. Chen, D. A. Delafuente, S. Sarangapani, T. E. Mallouk, *Catal. Today* **2001**, *67*, 341 – 355.
[287] D. Seley, K. Ayers, B. A. Parkinson, *ACS Comb. Sci.* **2013**, *15*, 82 – 89.
[288] H. B. Beer, *J. Electrochem. Soc.* **1980**, *127*, 303C – 307C.
[289] C. Comninellis, G. P. Vercesi, *J. Appl. Electrochem.* **1991**, *21*, 335 – 345.
[290] C. Comninellis, G. P. Vercesi, *J. Appl. Electrochem.* **1991**, *21*, 136 – 142.
[291] S. Trasatti, *Electrochim. Acta* **2000**, *45*, 2377 – 2385.
[292] J. Wu, Y. Xue, X. Yan, W. Yan, Q. Cheng, Y. Xie, *Nano Res.* **2012**, *5*, 521 – 530.
[293] Y. Gorlin, T. F. Jaramillo, *J. Am. Chem. Soc.* **2010**, *132*, 13612 – 13614.
[294] G. Li, H. Yu, X. Wang, S. Sun, Y. Li, Z. Shao, B. Yi, *Phys. Chem. Chem. Phys.* **2013**, *15*, 2858 – 2866.
[295] S. M. Hoseinieh, F. Ashrafizadeh, M. H. Maddahi, *J. Electrochem. Soc.* **2010**, *157*, E50 – E56.
[296] N. Cabrera, N. F. Mott, *Rep. Prog. Phys.* **1949**, *12*, 163 – 184.
[297] K. J. Vetter, F. Gorn, *Electrochim. Acta* **1973**, *18*, 321 – 326.
[298] R. Kirchheim, *Electrochim. Acta* **1987**, *32*, 1619 – 1629.
[299] M. Morita, C. Iwakura, H. Tamura, *Electrochim. Acta* **1978**, *23*, 331 – 335.
[300] F. Cardarelli, P. Taxil, A. Savall, C. Comninellis, G. Manoli, O. Leclerc, *J. Appl. Electrochem.* **1998**, *28*, 245 – 250.
[301] A. C. C. Tseung, S. Jasem, *Electrochim. Acta* **1977**, *22*, 31 – 34.
[302] P. Rasiyah, *J. Electrochem. Soc.* **1984**, *131*, 803 – 808.
[303] R. Kötz, S. Stucki, D. Scherson, D. M. Kolb, *J. Electroanal. Chem.* **1984**, *172*, 211 – 219.
[304] A. R. Zeradjanin, N. Menzel, P. Strasser, W. Schuhmann, *ChemSusChem* **2012**, *5*, 1897 – 1904.
[305] D. N. Buckley, L. D. Burke, *J. Chem. Soc. Faraday Trans. 1* **1975**, *71*, 1447 – 1459.
[306] D. N. Buckley, L. D. Burke, *J. Chem. Soc. Faraday Trans. 1* **1976**, *72*, 2431 – 2440.
[307] B. V. Tilak, V. I. Birss, J. Wang, C.-P. Chen, S. K. Rangarajan, *J. Electrochem. Soc.* **2001**, *148*, D112 – D120.
[308] S. Ardizzone, S. Trasatti, *Adv. Colloid Interface Sci.* **1996**, *64*, 173 – 251.
[309] J. A. Koza, Z. He, A. S. Miller, J. A. Switzer, *Chem. Mater.* **2012**, *24*, 3567 – 3573.
[310] M. W. Kanan, D. G. Nocera, *Science* **2008**, *321*, 1072 – 1075.
[311] M. W. Kanan, Y. Surendranath, D. G. Nocera, *Chem. Soc. Rev.* **2009**, *38*, 109 – 114.
[312] M. W. Kanan, J. Yano, Y. Surendranath, M. Dincă, V. K. Yachandra, D. G. Nocera, *J. Am. Chem. Soc.* **2010**, *132*, 13692 – 13701.
[313] C. L. Farrow, D. K. Bediako, Y. Surendranath, D. G. Nocera, S. J. L. Billinge, *J. Am. Chem. Soc.* **2013**, *135*, 6403 – 6406.
[314] E. R. Young, R. Costi, S. Paydavosi, D. G. Nocera, V. Bulović, *Energy Environ. Sci.* **2011**, *4*, 2058 – 2061.
[315] Y. Surendranath, M. Dincă, D. G. Nocera, *J. Am. Chem. Soc.* **2009**, *131*, 2615 – 2620.

[316] D. A. Lutterman, Y. Surendranath, D. G. Nocera, *J. Am. Chem. Soc.* **2009**, *131*, 3838 – 3839.
[317] M. Dincă, Y. Surendranath, D. G. Nocera, *Proc. Natl. Acad. Sci. USA* **2010**, *107*, 10337 – 10341.
[318] H.-Y. Su, Y. Gorlin, I. C. Man, F. Calle-Vallejo, J. K. Nørskov, T. F. Jaramillo, J. Rossmeisl, *Phys. Chem. Chem. Phys.* **2012**, *14*, 14010 – 14022.
[319] F. Jiao, H. Frei, *Energy Environ. Sci.* **2010**, *3*, 1018 – 1027.
[320] K. L. Pickrahn, S. W. Park, Y. Gorlin, H.-B.-R. Lee, T. F. Jaramillo, S. F. Bent, *Adv. Energy Mater.* **2012**, *2*, 1269 – 1277.
[321] M. Risch, A. Grimaud, K. J. May, K. A. Stoerzinger, T. J. Chen, A. N. Mansour, Y. Shao-Horn, *J. Phys. Chem. C* **2013**, *117*, 8628 – 8635.
[322] K. J. May, C. E. Carlton, K. A. Stoerzinger, M. Risch, J. Suntivich, Y.-L. Lee, A. Grimaud, Y. Shao-Horn, *J. Phys. Chem. Lett.* **2012**, *3*, 3264 – 3270.
[323] A. Grimaud, K. J. May, C. E. Carlton, Y.-L. Lee, M. Risch, W. T. Hong, J. Zhou, Y. Shao-Horn, *Nat. Commun.* **2013**, *4*, 2439.

